LBNL-42723

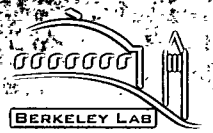

ERNEST ORLANDO LAWRENCE
BERKELEY NATIONAL LABORATORY

Seismicity and Crustal Structure at the Mendocino Triple Junction, Northern California

REC
MAR 29 1999
OSTI

Markus Dicke

Earth Sciences Division

December 1998

M.S. Thesis

DISCLAIMER

This document was prepared as an account of work sponsored by the United States Government. While this document is believed to contain correct information, neither the United States Government nor any agency thereof, nor The Regents of the University of California, nor any of their employees, makes any warranty, express or implied, or assumes any legal responsibility for the accuracy, completeness, or usefulness of any information, apparatus, product, or process disclosed, or represents that its use would not infringe privately owned rights. Reference herein to any specific commercial product, process, or service by its trade name, trademark, manufacturer, or otherwise, does not necessarily constitute or imply its endorsement, recommendation, or favoring by the United States Government or any agency thereof, or The Regents of the University of California. The views and opinions of authors expressed herein do not necessarily state or reflect those of the United States Government or any agency thereof, or The Regents of the University of California.

This report has been reproduced directly from the best available copy.

Available to DOE and DOE Contractors
from the Office of Scientific and Technical Information
P.O. Box 62, Oak Ridge, TN 37831
Prices available from (615) 576-8401

Available to the public from the
National Technical Information Service
U.S. Department of Commerce
5285 Port Royal Road, Springfield, VA 22161

Ernest Orlando Lawrence Berkeley National Laboratory
is an equal opportunity employer.

DISCLAIMER

Portions of this document may be illegible in electronic image products. Images are produced from the best available original document.

LBNL-42723

Seismicity and Crustal Structure at the Mendocino Triple Junction, Northern California

by

Markus Dicke

B.A. (University of California, Berkeley), 1997

A thesis submitted in partial satisfaction of the requirements for the degree of
Master of Science

in

Geophysics

in the

GRADUATE DIVISION
of the
UNIVERSITY of CALIFORNIA at BERKELEY

Committee in charge:

Professor Lane R. Johnson, Chair
Professor Douglas S. Dreger
Professor Alex Becker

This work was supported by the Office of Science, Office of Basic Energy Sciences, of the U.S. Department of Energy under Contract No. DE-AC03-76SF00098.

Abstract

Seismicity and Crustal Structure at the

Mendocino Triple Junction, Northern California

by

Markus Dicke

Master's of Science in Geophysics

University of California at Berkeley

Professor Lane R. Johnson, Chair

A high level of seismicity at the Mendocino triple junction in Northern California reflects the complex active tectonics associated with the junction of the Pacific, North America, and Gorda plates. To investigate seismicity patterns and crustal structure, 6193 earthquakes recorded by the Northern California Seismic Network (NCSN) are relocated using a one-dimensional crustal velocity model. A near vertical truncation of the intense seismic activity offshore Cape Mendocino follows the strike of the Mattole Canyon fault and is interpreted to define the Pacific plate boundary. Seismicity along this boundary displays a double seismogenic layer that is attributed to interplate activity with the North America plate and Gorda plate. The interpretation of the shallow seismogenic zone as the North America - Pacific plate boundary implies that the Mendocino triple junction is situated offshore at present. Seismicity patterns and focal mechanisms for events located within the subducting Gorda plate are consistent

with internal deformation on NE-SW and NW-SE trending rupture planes in response to north-south compression. Seismic sections indicate that the top of the Gorda plate locates at a depth of about 18 Km beneath Cape Mendocino and dips gently east- and southward. Earthquakes that are located in the Wadati-Benioff zone east of 236°E show a change to an extensional stress regime indicative of a slab pull force. This slab pull force and scattered seismicity within the contractional forearc region of the Cascadia subduction zone suggest that the subducting Gorda plate and the overriding North America plate are strongly coupled. The 1992 Cape Mendocino thrust earthquake is believed to have ruptured a blind thrust fault in the forearc region, suggesting that strain is accumulating that must ultimately be released in a potential M 8+ subduction earthquake.

Contents

List of Figures

List of Tables

Chapter 1

Introduction

The Mendocino Triple Junction plays a pivotal role in the complex framework of active tectonics in the northeastern Pacific Ocean. It is the location in Northern California where three plates, the North American, the Pacific, and the Juan de Fuca-Gorda Plate, intersect and interact.

The kinematic evolution of the Mendocino triple junction and its significance to the geological development of western North America have been recognized since the earliest proposals of the theory of plate tectonics in the 1960's. The junction defines the northern termination of right-lateral motion between the North American and Pacific plate along the complex San Andreas Fault System. To the west, plate motion between the Pacific and Juan de Fuca-Gorda plate system is accomodated along the east-west trending Mendocino Fracture zone, a right-lateral transform fault. To the north, active subduction of the Juan de Fuca-Gorda plate occurs along the

Cascadia Subduction zone (Figure 1.1). The theory of plate tectonics provides the basis to postulate a time-history of the Mendocino triple junction and shows that it has migrated northward along the California coastline to its current location during the past 25 Ma. These general kinematics and their implications to the geological evolution of western North America have been recognized and are widely accepted [McKenzie and Morgan, 1969; Atwater, 1970; Dickinson and Snyder, 1979].

Fundamental to the understanding of active tectonics at the Mendocino triple junction is the definition of plate boundaries. The exact location of the triple junction near Cape Mendocino is not well determined at present, due to the structural complexity of the region. The present debate whether the junction is located offshore, as traditionally assumed, or onland to the southeast of Cape Mendocino, as proposed by McLaughlin et al. [1994], remains unresolved. Thus, to refine the delineations of the present-day geometry and to provide a better understanding of the inter- and intraplate processes, a refined structural model of plate geometries is required.

Resolving the large-scale three-dimensional plate geometry can also provide insight into the stability of the plate configuration. The Mendocino triple junction constitutes a fault-fault-trench (FFT) triple junction that is currently in an unstable configuration: a FFT triple junction is considered unstable if the trench (here the Cascadia subduction zone) and the fault (here the San Andreas) do not lie on a small circle, because it cannot retain its geometry as the plates move [McKenzie and Morgan, 1969]. How this instability is acommodated at the intersection of the

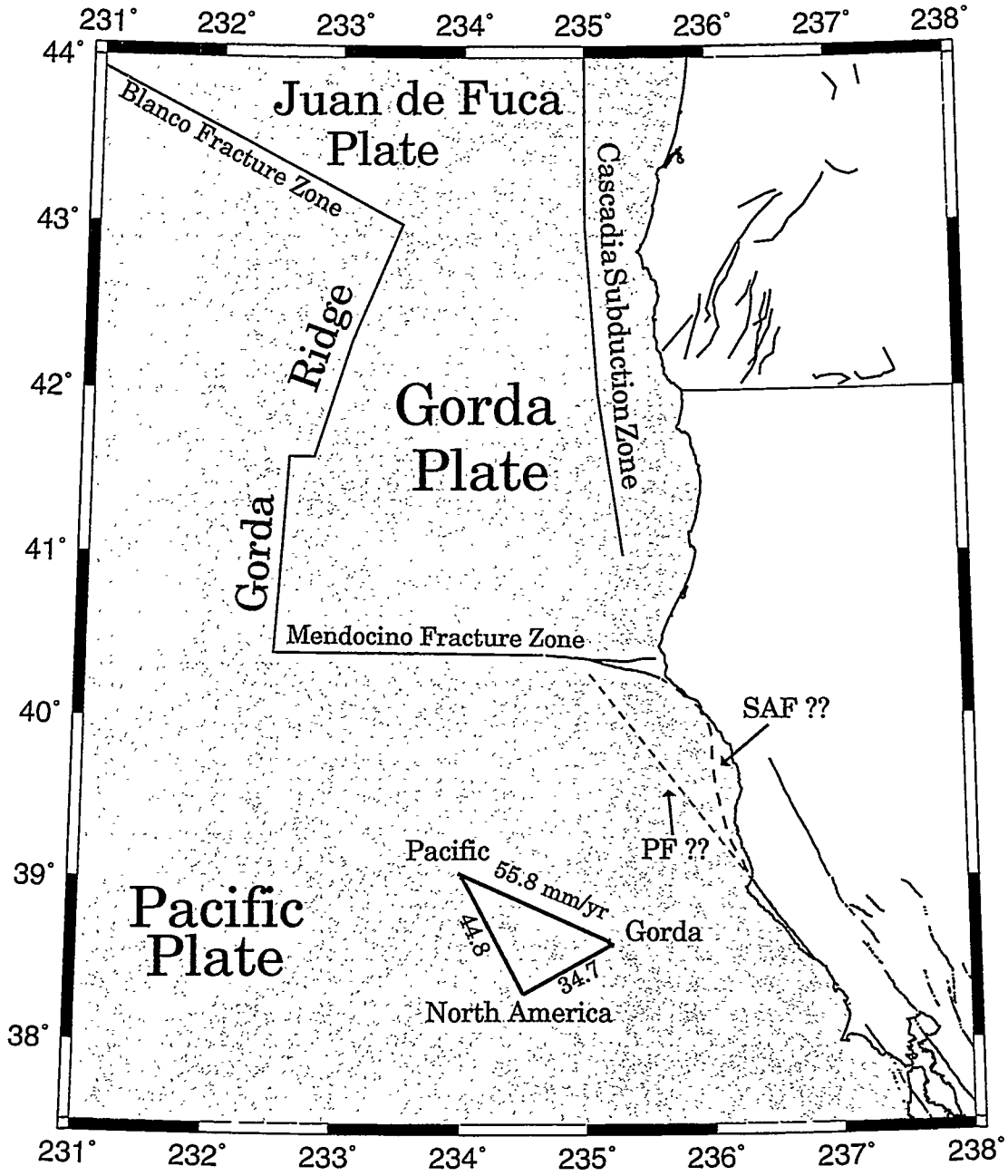

Figure 1.1: Generalized map of tectonic features in Northern California. The velocity diagram (triangle vector diagram) shows the relative motions between the Pacific, North American and Gorda plates at the location of the triple junction. SAF, San Andreas fault; PF, Pilarcitos fault (proposed by Griscom and Jachens [1989]). Figure 1.2 shows a magnified view of the area near Cape Mendocino.

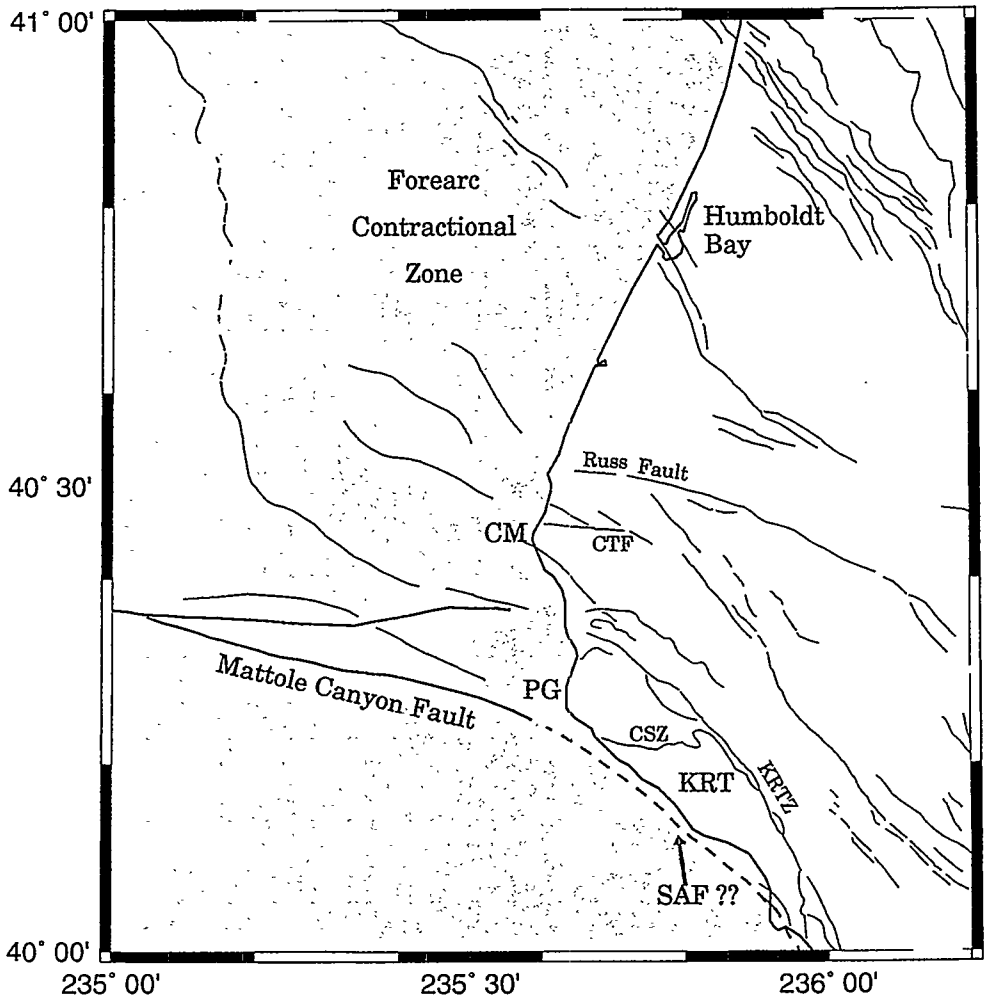

Figure 1.2: Magnified view of the study area at the Mendocino triple junction. Map shows the location of important geographical features that are discussed in this study. SAF, San Andreas fault; KRT, King Range terrane; KRTZ, King Range thrust zone; CSZ, Cooskie shear zone; PG, Punta Gorda; CM, Cape Mendocino; CTF, Capetown fault.

plates near Cape Mendocino is not understood. In particular, it is not known how the San Andreas fault, the Mendocino fault, and the Cascadia subduction zone intersect at the Mendocino triple junction. Defining the plate boundaries within this region should be useful in solving these enigmas.

The purpose of this study is the analysis of present day seismicity at the Mendocino triple junction and to deduce a three-dimensional crustal structure. Intense seismic activity at the triple junction accounts for more than 25% of seismic energy released within California over the past 50 years [Gee et al., 1991]. This activity, in combination with the triple junction's proximity to a land based seismic network, provides an unique opportunity to investigate plate geometries and interplate processes in this region. Reliable hypocenter locations are determined for over 6000 earthquakes which occured over the time period between 1974 and 1998 at the Mendocino triple junction. Additionally, focal mechanisms are utilized to interpret the distribution of seismicity in terms of inter- and intraplate activity and to characterize the style of faulting in the region.

This study gives special attention to several large earthquake sequences that define the primary mode of deformation within the tectonic plates and along their boundaries. In particular, the 25 April 1992, M_S=7.1 Cape Mendocino thrust earthquake is of great importance for the region as it is the first well-recorded event that is associated with relative plate convergence of the Gorda and North American plates. The study discusses the implications of over 1500 recorded aftershocks of this event for

the definition of plate boundaries and the degree of coupling between them. Other earthquake sequences are investigated to demonstrate the extent of internal faulting, which is the primary mode of deformation within the Gorda plate.

An improved understanding of active tectonics at the Mendocino triple junction is essential in the assessment of earthquake hazard for Northern California. Chapter Two of this study provides a general overview of the tectonic setting of Northern California and summarizes the tectonic evolution of the triple junction. In Chapter Three, the methodology of relocating earthquakes is described and results of the procedure are presented. The analysis focuses on the regional distribution of earthquakes as well as on the importance of "reference" earthquakes for the definition of the triple junction geometry. The results are discussed in Chapter Four, with the emphasis on the present configuration and state of the Mendocino triple junction. The conclusions and their implications for earthquake hazards in the vicinity of Cape Mendocino are presented at the end of chapter Four.

Chapter 2

Tectonic Overview

2.1 Introduction

The evolution of the Mendocino triple junction (MTJ) is driven by the relative plate motions of the North America, the Juan de Fuca-Gorda and the Pacific plate. Since its creation in the Oligocene due to the relative convergence of the North America and Pacific plates, the triple junction has migrated northward along the western North-America plate boundary, resulting in a growing San Andreas fault system and continuously shaping the geological structure of the entire western U.S. Additionally, the internal deformation of the subducting Gorda plate to the north of the MTJ has affected the development in time and space and added to the complexity of the plates' junction. It is therefore logical to present the tectonic overview of the Mendocino triple junction in terms of the plates' characteristic behavior.

This chapter summarizes the tectonic evolution of the MTJ inferred from numerous studies. These studies have focused on tectonics, gravity modeling, reflection profiling, seismicity, seafloor magnetic anomalies, and coastal geology. Since it is not clear how the plates interact at the location of the triple junction, an investigation how the junction developed in the past helps in understanding their present nature. This is accomplished by analyzing the San Andreas fault system and its tectonic history, as it is a direct consequence of the northward migrating triple junction. Seafloor magnetic anomalies recorded in the oceanic crust of the Gorda plate are used to deduce relative plate motions in the past. Lastly, evidence is gathered that relates to the question whether subduction of the Juan de Fuca-Gorda plate has occured seismically or aseismically during the Holocene.

2.2 Creation of the Mendocino Triple Junction

The Mendocino triple junction was created about 25 Ma ago as a result of relative plate motions. In what was soon acknowledged as a landmark study of the theory of plate tectonics, Atwater [1970] and Atwater and Molnar [1973] used magnetic anomaly patterns in the northeast Pacific Ocean to reconstruct the tectonic evolution of western North America. A spreading ridge, the ancestral east-Pacific rise, existed in the north-eastern Pacific Ocean during mid-Teriary and formed new oceanic crust as the Pacific and the ancestral "Farallon plate" (after McKenzie and Morgan [1969])

drifted away to the west and east of this ridge, respectively (Figure 2.1a). There also existed a subduction zone along the western margin of the North America plate that consumed the Farallon plate. Eventually, the east-Pacific rise encountered the subduction zone (the rate of subduction was greater than the rate of creation at the ridge), at which point the San Andreas transform was generated with a pair of triple junctions at either end (Figure 2.1b). The remaining subplates of the once intact Farallon plate continued subducting beneath North America to the north and south of these triple junctions. This process has continued up to the present, as the Juan de Fuca/Gorda plate subducts along the Cascadia subduction zone (CSZ) north of the Mendocino triple junction and the Rivera plate south of the homonymous triple junction at the transforms southern termination.

An effect of Neogene tectonics has been to lengthen the transform boundary between the Pacific plate and North America as the Mendocino and Rivera triple junctions migrate in opposite directions. Although this model gives a simplified view of neotectonics along the western North American margin, the evolution is much more complicated in detail. In particular, the dynamic processes by which the northward migrating MTJ terminates active subduction of the Cascadia subduction zone and initiates transform shear on the San Andreas fault (SAF) are not understood. A characterization of the evolution gets further complicated by the fact that plate geometries at a triple junction must satisfy certain conditions to maintain a stable configuration. There is evidence that during its evolution as well as at present the Mendocino triple

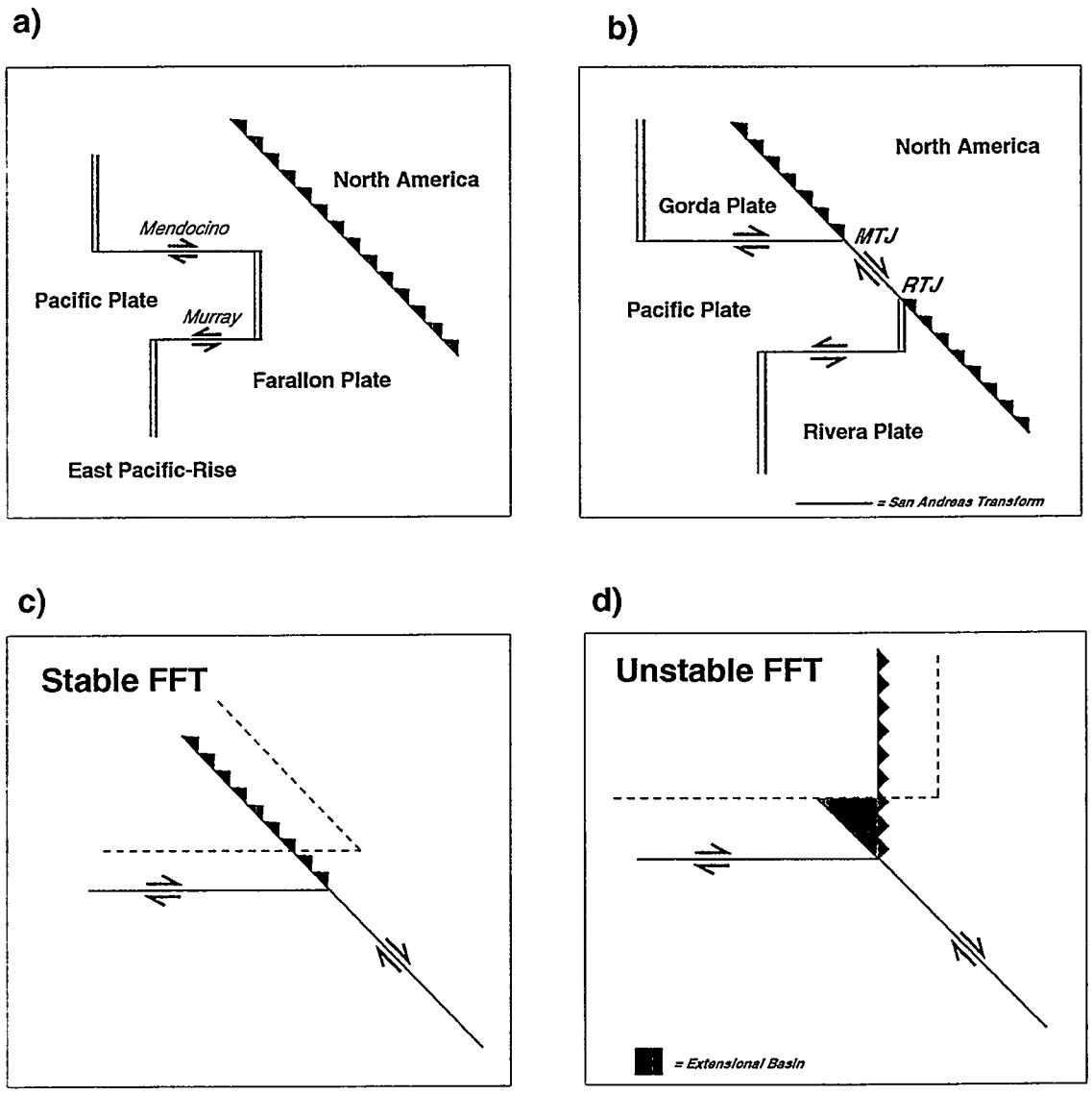

Figure 2.1: Creation and stability of the Mendocino triple junction. (a) Initial configuration of the East-Pacific rise, transforms, and the subduction zone along the continental margin. (b) Configuration some time after the East-Pacific rise had encountered the trench. The Mendocino (MTJ) and Rivera (RTJ) triple junctions migrate away from each other, thereby lengthening the San Andreas transform in between. (c) Condition on the plate configuration of a fault-fault-trench (FFT) triple junction to be stable. The dashed line shows the same plate boundaries after some time-period. The triple junction migrates northward, yet does not alter the geometry of the plate boundaries. (d) Plate configuration for an unstable FFT triple junction. The trench and the tranform are not collinear. As the plates continue their relative motions, an extensional basin results.

junction has experienced transient instabilities.

2.3 Stability of the Mendocino Triple Junction

The geometry of the Pacific, the Gorda and the North America plate and their relative velocities implies an unstable triple junction configuration. Shortly after the postulation of the theory of plate tectonics, McKenzie and Morgan [1969] investigated all possible plate geometries that result in triple junctions and their evolution through time. According to their definition, a stable triple junction is one that can retain its geometry as the plates move. Thus, certain restrictions on the orientation of plate boundaries for stable triple junctions apply. In the case of a fault-fault-trench (FFT) triple junction such as the Mendocino, a stable geometry can exist only if the trench and the fault are collinear, thus defining a small circle (Figure 2.1c).

Dickinson and Snyder [1979] investigated the plate configuration and their effects on the stability of the Mendocino triple junction. Inspection of present day plate geometries off the Pacific northwest coast indicates that the Cascadia subduction zone does not lie on a small circle with the San Andreas transform (e.g. Dickinson and Snyder [1979], their Figure 1). Figure 2.1d displays a simplified, though exaggerated diagram of the unstable plate configuration. The trench (here the CSZ) trends more northerly than the fault (here the SAF) which results in the formation of an area that experiences extensional deformation as the plates continue their motions. Dickinson

and Snyder [1979] interpret several large sedimentary basins of Cenozoic age along the California coastline as an indication of transient instabilities of the MTJ at the time of passage.

Another source for instability is provided by the fact that the Mendocino and Rivera triple junctions diverge along the convex contintental margin of North America. The North American plate displays an oceanward bulge along its westcoast, for which a readjustment of the newly created transform boundary (the SAF) would be expected as the triple junctions migrate away from each other. This adjustment would be accomplished by an eastward step of the transform fault, thereby carving a band out of the North American crust and accreting it to the Pacific plate. Griscom and Jachens [1989] argue that such a process would be possible due to the relatively thin lithosphere and the thermal regime along the continental margin. The question arises whether scientific evidence exists along the San Andreas transform that would prove this hypothesis.

2.4 The San Andreas Transform

There is substantial evidence suggesting that the present San Andreas fault has **not** been the master slip surface between the Pacific and North America plate for the entire time span. Lateral offsets of similar geological features along the present trace of the San Andreas fault are reported to be approximately 300 Km [Hill and Dibblee,

1953; Graham and Dickinson, 1978; Dickinson and Snyder, 1979; Stanley, 1987], well short of the postulated maximum slip expected from calculations of relative plate motions between Pacific and North American plates (ca. 800 Km over the past 25 Ma [Atwater and Molnar, 1973]). This implies that the principal slip surface prior to about 5 Ma must have been to the west of the San Andreas, presumably along the terminated trench.

There seems to be evidence that the principle slip surface repeatedly shifted eastward from its original location along the continental margin. In addition to the approximately 300 Km of offset along the San Andreas fault, Graham and Dickinson [1978] measured a total offset of 105 Km along the San Gregorio-Hosgri fault. This fault trends parallel to the continental slope offshore central California and joins the San Andreas fault just north of San Francisco. Furthermore, interpretation of gravity and magnetic anomaly data by Griscom and Jachens [1989] led to the proposal that slip along an inferred extension of the Pilarcitos fault north of Point Arena (see Figure 1.1) shifted towards the present San Andreas trace at about 5 Ma ago. However, the existence of such a northward extension has not been proven, yet it might explain a lateral offset of ca. 130 Km between the continental shelves to the north and south of the Mendocino fracture zone.

The modern kinematics of the San Andreas fault system in northern California may support the proposed neotectonic evolution. Furlong et al. [1989] point toward thermal-mechanical processes associated with the northward migrating triple junction

to be responsible for the eastward shift of the San Andreas. Relatively young (2-4 Ma) faults to the east of the San Andreas fault, such as the Hayward and Calaveras faults and their northward extensions along the Maacama fault zone, currently accomodate a significant fraction of plate motion. This may indicate continuous eastward stepping behavior of the transform boundary initiated by the northward migration of the Mendocino triple junction. Consequently, eastward transformation of the principle slip "system" implies accompanying eastward jumps of the triple junction itself [Griscom and Jachens, 1989]. Therefore, neogene evolution of the Mendocino triple junction seems to be characterized by periods in which the geometry of the three plates led to instabilities of the system.

2.5 The Non-rigid Gorda plate

Internal deformation of the subducting Gorda plate indicates non-rigid plate behavior. From seismicity and magnetic anomaly studies it has been concluded that internal deformation results from motions of the surrounding plates. There is general agreement that north-south compression is accomodated along north-east striking, left-lateral transform faults within the plate. However, the kinematics and mechanisms of the deformation are controversial and not well resolved.

Time- and space-varying spreading along the Gorda ridge is responsible for the internal Gorda plate deformation. Raff and Mason [1961] first mapped and noticed strong curvatures in magnetic lineations to the east of the Gorda ridge. Addition-

ally, Silver [1971] noticed that these lineations are tens of kilometers shorter than their counterparts on the western half of the ridge. These patterns result from a change in relative plate motions between the Juan de Fuca/Gorda and Pacific plates that caused a clockwise ridge and plate rotation [Carlson, 1976, 1981; Riddihough, 1980, 1984]. Furthermore, a southward decrease in spreading rates along the Gorda ridge [Riddihough, 1980; Wilson, 1989] and decreasing rates in time [Wilson, 1986] define deviations from rigid plate motions. As a consequence of these changes, a "space-problem" exists for the Gorda plate as the Blanco and Mendocino Fracture zones no longer trend parallel (Figure 1.1) and convergence between the Juan de Fuca and Pacific plates is initiated. Without any evidence for subduction along the Mendocino fault [Jachens and Griscom, 1983; Wilson, 1986; McPherson, 1989; Smith et al., 1993], the space-problem is accommodated within the Gorda plate since it is the youngest and, thus, weakest within the system.

Internal deformation of the Gorda plate manifests itself in a broad and diffuse area of seismicity. Early seismicity studies by Bolt et al. [1968] and Simila et al. [1975] interpreted strike-slip mechanisms in the Gorda basin as right-lateral, northwest striking transforms that would transfer motion from the San Andreas fault across the Gorda Basin to the Blanco Fracture zone. However, several large intraplate earthquakes, i.e. the November 8, 1980 Eureka earthquake [Eaton, 1981], reveal fault planes striking northeasterly, suggesting left-lateral motion [Smith and Knapp, 1980; Smith et al., 1981]. This interpretation follows Silver's [1971] proposition that deformation within

the Gorda crust occurs on left-lateral, northeast striking faults parallel to magnetic anomalies and along lines of original mechanical weakness. Although shear motion along northeast striking faults are now considered to be the primary mode of internal deformation, it cannot solely explain the shortened magnetic anomalies [Wilson, 1989]. At present, the kinematic evolution of the "Gorda deformation zone" and its transition into rigid plate behavior towards the Juan de Fuca plate is a topic of intense discussions, yet beyond the scope of this study.

The highest concentration of seismicity in the Gorda plate is located in the vicinity of the Mendocino triple junction. The buttressing effect of the Pacific plate [Smith et al., 1993] is inferred to be greatest in this area. However, not all seismic activity can be attributed to the internal deformation of the Gorda plate, and some must be due to the complex interactions between the three plates. Of particular interest is the question of the nature of relative motion between the Gorda and North America plate at the southern termination of the Cascadia subduction zone (coseismic, aseismic or no present motion).

2.6 Subduction of the Gorda plate

It was recently suggested that the Gorda plate exhibits coseismic slip during subduction beneath the North American plate. These studies exposed problems with earlier interpretations that the relative motion between the Gorda and North America plate trends parallel to the subduction zone [Riddihough, 1980; Riddihough, 1984]

and that the Gorda plate may be subducting aseismically [Heaton and Kanamori, 1984]: the 25 April, 1992 Cape Mendocino thrust earthquake (M_s=7.1) is interpreted to have relieved strain due to the convergence of the two plates [Oppenheimer et al., 1993; Murray et al., 1996]; furthermore, paleoseismicity studies [Clarke and Carver, 1992; Merrits, 1996] found evidence for large subduction-related events in the Holocene that would indicate strong coupling. Spence [1989] supports this conclusion based on stress calculations throughout the Cascadia plate system.

The geometry of the Gorda plate beneath northern California has been inferred from several geophysical investigations. East of the Mendocino triple junction, Jachens and Griscom [1983] inferred the southern edge of the Gorda plate to trend 120°N for about 120 Km, after which it changes to an easterly direction. This southeasterly trend reflects the direction of Gorda plate motion parallel to the Blanco Fracture zone while the change in strike further inland correlates well in time with the change of plate motion described in chapter 2.5. An eastward dip of approximately 10° for the downgoing slab is reported by various studies [Jachens and Griscom, 1983; Cockerham, 1984; McPherson, 1989; Smith et al., 1993; Verdonck and Zandt, 1994]. Further inland, the downgoing slab was imaged at depths up to 270 Km [Benz et al., 1992], with remnants of the ancestral Farallon plate even as deep as 400 Km [Romanowicz, 1980].

2.7 Relative Plate Motions

Relative velocities of the Pacific, North America and Gorda plates at the Mendocino triple junction can be displayed in velocity space. The NUVEL-1A global plate motion model [DeMets et al., 1990] provides the directions and velocities of these plates to each other (see Figure 1.1): motion between the Pacific plate relative to North America is 44.7 mm/a trending N27.5^{0}W; relative motion between the Gorda and Pacific plates is assumed to be 55.8 mm/a at 114°N, however, this estimate may involve some problems, since the Gorda plate is deforming internally; given these assumptions and closing the vector triangle yields a relative convergence rate between the Gorda and North American plate of 34.7 mm/a at an azimuth of 240.8°N.

In summary, the tectonic evolution of the Mendocino triple junction has been dictated by the relative motions of the Pacific, North America and Gorda plates. The stability of the triple junction in the past seems to have been characterized by the geometry at the intersection of the plates. In the following chapter, seismologic data is presented and analyzed with the intention to resolve the uncertainties in plate geometry at the Mendocino triple junction.

Chapter 3

Seismicity Data

3.1 Introduction

The primary focus of this study is the analysis of present seismicity at the Mendocino triple junction. As one of the seismically most active regions in western North America, it has produced more than 60 earthquakes over the past century that caused damage in the vicinity of Cape Mendocino [Dengler et al., 1992]. Since 1974, over 12500 events with magnitudes ranging from 0.5 to 7.1 were recorded and provide the data used in this study. Phase arrival times are retrieved for events between longitudes 235°E and 237°E and latitudes 39.8°N and 42.0°N from the Northern California Seismic Network (NCSN) catalog. Figure 3.1 displays the histogram of the seismicity during the time period between July 1974 and October 1998.

The seismic activity at the Mendocino triple junction since 1974 is characterized

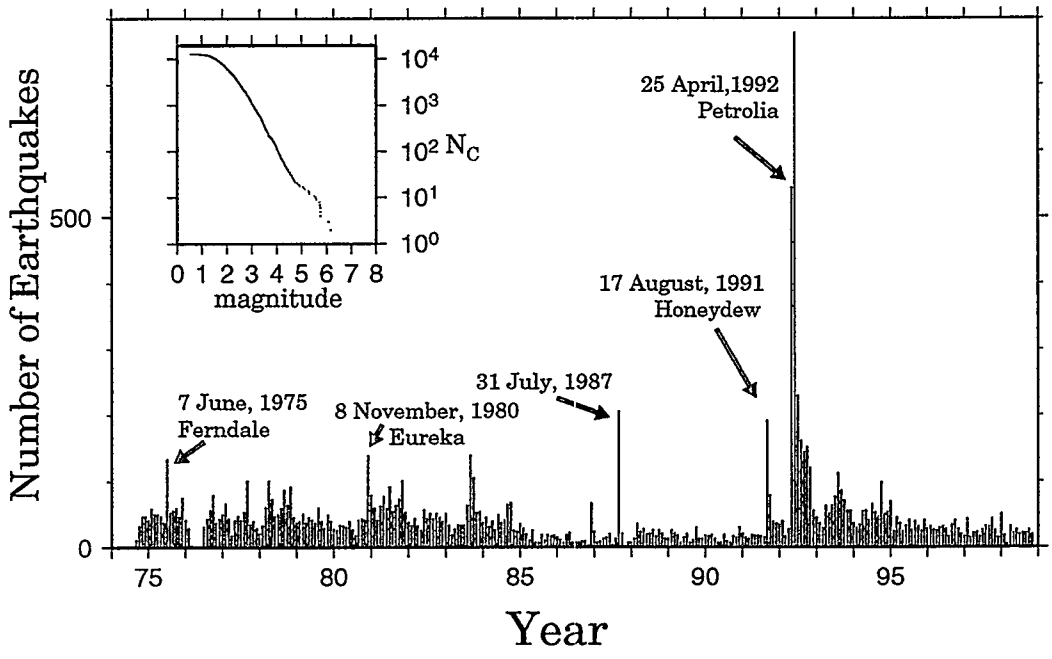

Figure 3.1: Monthly seismicity from July 1974 through October 1998 for the region between longitudes 235°E and 237°E and latitudes 39.8°N and 42.0°N. Inset shows the cumulative number of events as a function of event magnitude.

by a continuous background level of microseismicity and several large events. The most prominent feature in Figure 3.1 is the occurence of the 25 April, 1992, Cape Mendocino earthquake and its aftershock sequence. This event plays a major role in the investigation of plate configurations at the triple junction since more than 1500 recorded aftershocks are included in this sequence. Other significant events for the region under investigation include the 1975 Ferndale (M_D=5.2), the 31 July, 1987, M=5.6 and the 17 August, 1991, Honeydew earthquake (M_S=7.1).

In the following sections, 24 years of seismicity at the Mendocino triple junction will be analyzed. The recorded earthquakes are relocated and their temporal and spatial distribution is investigated with respect to present-day plate geometries. Focal

mechanisms are determined using seismograms recorded at stations of the Berkeley Digital Seismic Network (BDSN). The results reflect the complexity associated with the geometry and the relative plate motions of the North America, Pacific and Gorda plates.

3.2 Estimation of Hypocentral Parameters

3.2.1 Station Network

The network of seismic stations used in this study consists of 84 short period stations in coastal northern California and southern Oregon (Figure 3.2a). The majority of stations are operated by the U.S. Geological Survey (USGS) as a result of a network expansion in 1980. Additional data are provided by stations of the TERA Corporation operated in the Humboldt Bay region between 1974 and 1986, stations of the BDSN and a station operated by the California Division of Water Resources (DWR). During a 2-month period following the 8 November, 1980, M_s=7.2 Eureka earthquake, a temporary network of portable seismometers improved the station coverage of the region.

The stations displayed in Figure 3.2a are selected to provide maximum azimuthal coverage of the area under investigation. Most of the earthquakes at the triple junction occur offshore Cape Mendocino, outside the land-based network. Without the use of ocean bottom seismometers, azimuthal coverage must be optimized onshore in order

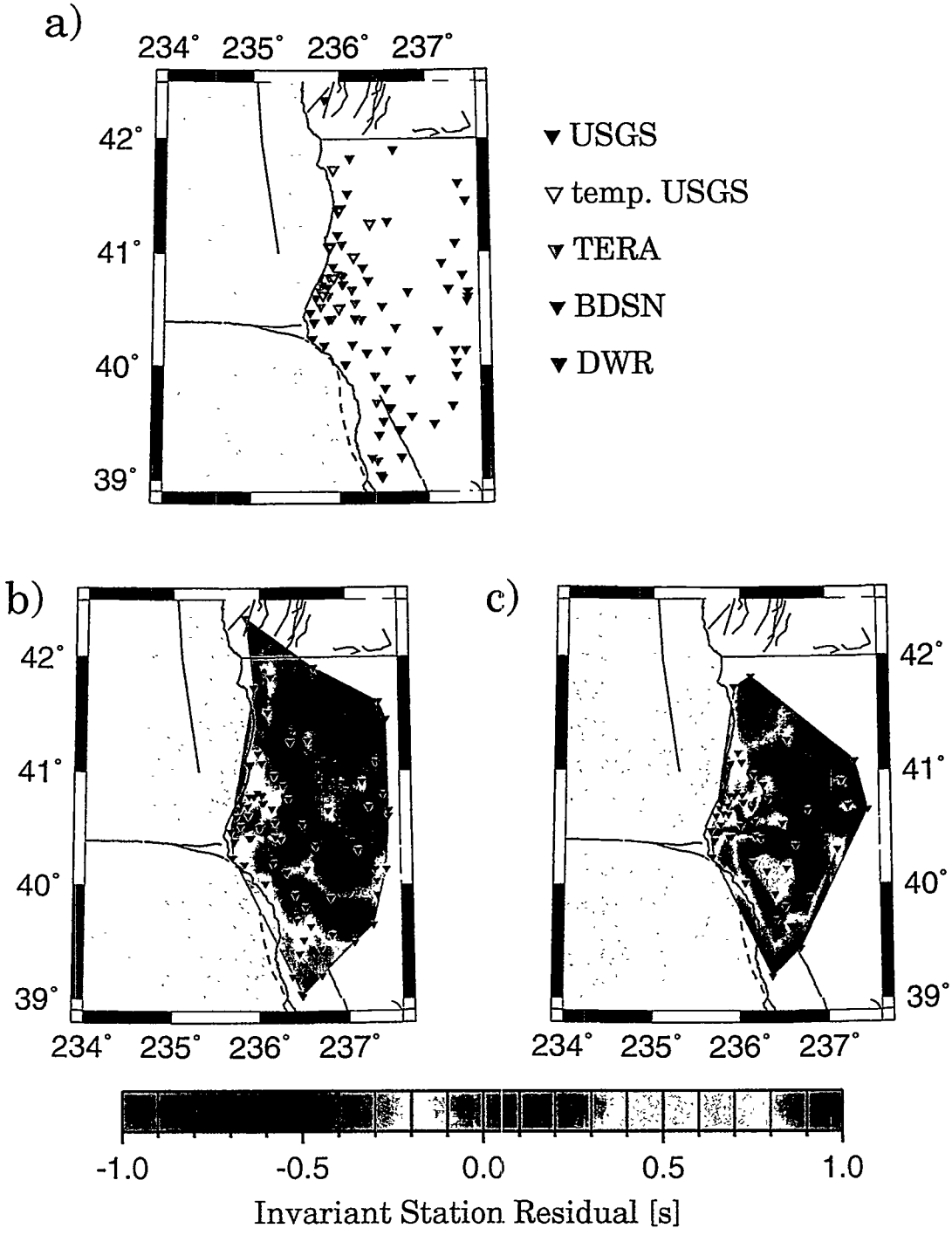

Figure 3.2: (a) Map showing the array of seismographic stations of this study. Contour maps of the "invariant" portion of the residual (independent of azimuth and angle of incidence) for P- (b) and S-waves (c).

to get relieable hypocentral estimates for these events. Previous investigations on the seismicity at the triple junction [Smith and Knapp, 1980; Cockerham et al., 1989; McPherson, 1989; Smith et al., 1993] exclusively used data recorded by the TERA network. This study incorporates the same data within the larger network shown in Figure 3.2a, therefore effectively increasing the network's aperture. However, the area spanned by the network must remain within the bounds where the applied velocity model is valid.

3.2.2 Velocity Model

The velocity model used to locate earthquakes in the Mendocino triple junction region reflects the geology of the Northern California Coast Ranges. The Coast Ranges are underlain by the Franciscan Complex, an uplifted accretionary wedge that formed during the Mesozoic and early Tertiary [Jachens and Griscom, 1983; Castillo and Ellsworth, 1993]. Forearc metasedimentary and metavolcanic rocks, granitic plutons and Tertiary volcanic rocks are typical for the Coast Ranges and Klammath Mountains [Benz et al., 1992]. Beneath the northern Coast Ranges, the crustal thickness is believed to be approximately 24 Km [Oppenheimer and Eaton, 1984], and thickening to the northeast. This crustal structure is approximated by the one-dimensional, layered velocity model Gil7 [Dreger and Romanowicz, 1994]. The same model is currently used by the University of California Berkeley Seismological Laboratory in moment tensor inversions of three-component waveforms (e.g. Pasyanos et al. [1996]).

Table 3.1: Parameters of the Gil7-velocity-model

Depth (Km)	v_p (m/s)	v_s (m/s)	ρ (Kg/m^3)
0.0	3200	1500	2280
1.0	4500	2400	2280
3.0	4800	2780	2580
4.0	5510	3180	2580
5.0	6210	3400	2680
17.0	6890	3980	3000
25.0+	7830	4520	3260

The velocity parameters of the Gil7-model are listed in Table 3.1.

The validity of the velocity model can be further improved by incorporating travel time corrections for each station to account for local inhomogeneities that are likely to exist within the area of the seismic array. In particular, station elevation and surface geology are variable throughout the region and constitute "velocity anomalies" in the shallow crustal structure. Since all rays must travel through the same shallow structure to reach a particular station, the corresponding station delay was calculated as the average travel time residual from a high-quality subset of events. Figures 3.2b and c show contour maps of the average station residuals for P- and S-waves, respectively. Note that S-wave residuals are only applied at stations that recorded a minumum of 5 S-phases for events of the subset. A comparison of station residuals with station elevations indicates a close correlation (i.e. stations within the Coast Ranges). Positive residuals for stations in the Eel River Basin just north of Cape Mendocino (Figure 3.2) are found to correlate well with the surface geology since it describes a sediment filled basin ca. 3 Km deep [Ogle, 1953]. Table A.1 of the

appendix gives a complete list of station location, elevation and corresponding travel time corrections.

3.2.3 Location Method

Out of the 12500 recorded events in the vicinity of the Mendocino triple junction, a subset of 9362 events had P-arrival times recorded at a minimum of ten different stations. Hypocenter locations and origin times are estimated for these events by a program that minimizes the sum of the squares of residuals. Travel times are calculated by tracing rays through the one-dimensional Gil7 velocity model. The program starts with the initial location from the NCSN-catalog and iteratively searches for the best-fit location. Although S-phase readings are not required in the location procedure, their incorporation is advantageous as they improve hypocentral estimates, particularly for offshore events. P- and S-phases are weighted separately: P-wave recordings are fully weighted (1.00), while S-waves are weighted by the ratio of the seismic-wave velocities (0.577). In addition to earthquake locations, focal mechanisms are obtained for selected events to constrain fault plane orientations. Focal mechanisms are determined using a moment tensor inversion method that is based on complete waveform modeling. The program utilizes three-component, long-period (10-100s) displacement waveforms recorded at stations of the BDSN. The six independent elements of the moment tensor are inverted for by fitting synthetic waveforms to the recorded seismograms. Additional source mechanisms are obtained from the

moment tensor catalog at the Berkeley Seismological Laboratory [Dreger, 1998] and various other publications (e.g. Velasco et al. [1994], Oppenheimer et al. [1993]).

3.3 Results of Earthquake Relocations

3.3.1 Overview

The results of the relocated seismicity at the Mendocino triple junction reflect the complexity of the plate geometries. Figure 3.3 displays the epicenters of 6193 earthquakes for which "reliable" locations were determined. Reliable locations are defined by root-mean-square (rms) residuals of less than 0.5 seconds. The average rms residual for this subset of events is 0.22 seconds and uncertainties in the hypocentral location are less than 2 Km in the horizontal and less than 3 Km with depth. Events with rms residuals greater than 0.5 s are not suited for the purpose of this study as their uncertainties in hypocentral parameters become greater than these values.

The map view in Figure 3.3 illustrates the spatial distribution of seismicity at the Mendocino triple junction. The most obvious feature is the area of dense seismicity in the near and offshore region of Cape Mendocino. The abundance of earthquakes in this region has long been recognized [Bolt et al., 1968; Simila et al., 1975; Smith and Knapp, 1980; McPherson, 1989; Smith et al., 1993] and corresponds to tectonic activity at the triple junction. Finite-element modeling by Jachens and Griscom [1983] and strain-rate modeling by Wilson [1986] predict this to be the area of maximum

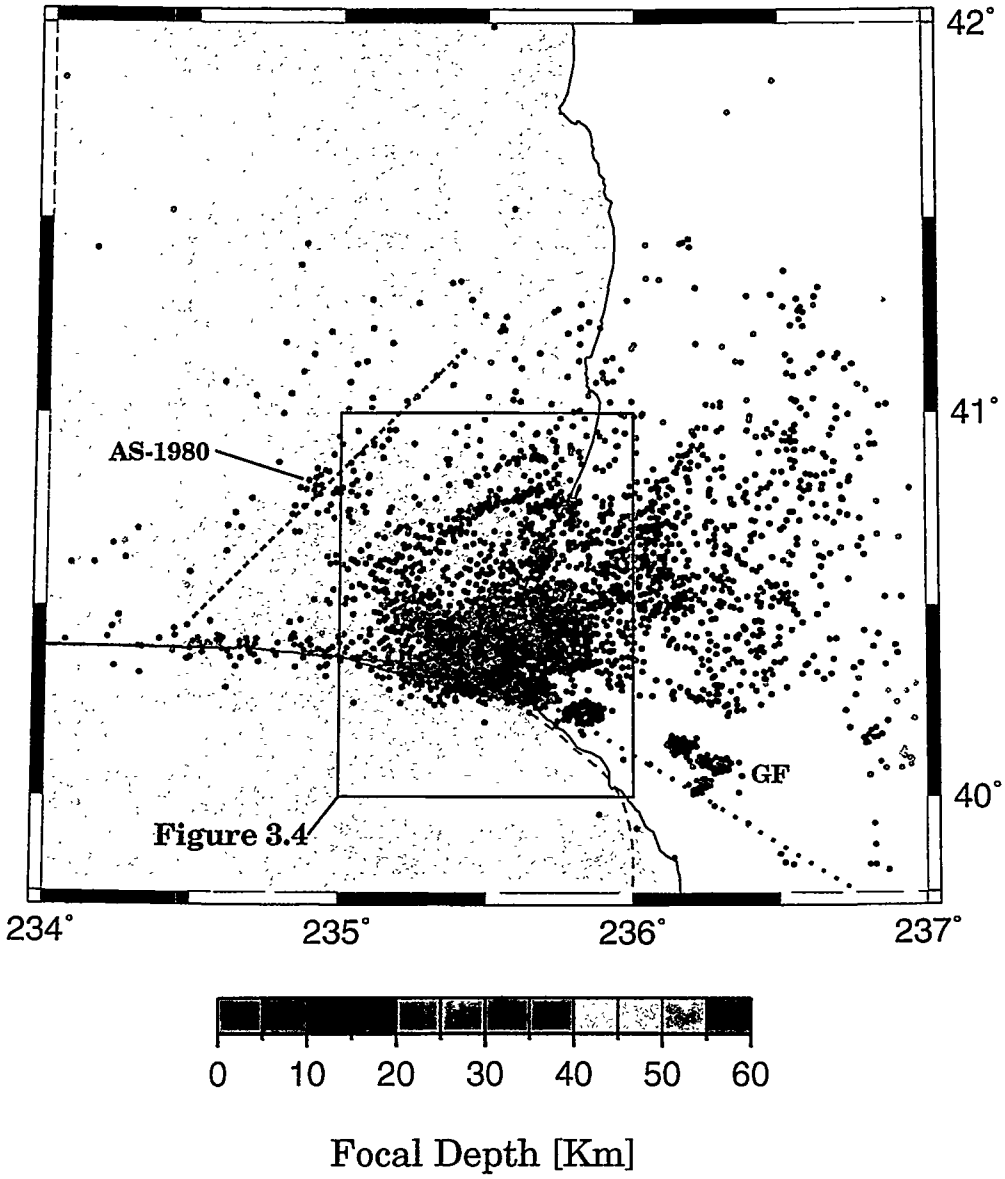

Figure 3.3: Map of seismicity at the Mendocino triple junction 1974-1998. Colors correspond to depth of event; each circle represents a single event, not scaled to magnitude. Black dashed line shows the aftershock zone of the 1980 Eureka earthquake. Red dashed line is the surface projection of the southern edge of the Gorda plate [after Jachens and Griscom, 1983]. Note that seismicity west of 235° is not complete (see text for explanation). GF, Garberville Fault.

compressive stresses at the triple junction. Although it is impossible to recognize any patterns or lineations within this "cloud" of events, it is noticeable that the hypocenters range in depth from near the surface to more than 40 Km, indicating that brittle failure occurs at greater depths than is usual in the continental crust of California.

Several northeast-southwest trending lineations of events can be observed offshore of Humboldt Bay to the north of the intense cloud. The depth range for these events suggests that they are caused by internal deformation of the Gorda plate on NE-trending, left-lateral faults as was proposed by Silver [1971]. Interestingly, these lineations are nearly parallel to a 120 Km fault segment that ruptured during the 8 November, 1980, Eureka earthquake (Figure 3.3). The occurence of that event confirmed Silver's [1971] suggestion of left-lateral, internal deformation of the Gorda plate. Several events marked as "AS-1980" (Figure 3.3) are relocated as part of this study and identified as aftershocks of the 1980 earthquake.

The results of relocating the 1980 aftershocks and other events has significant implications on the location procedure. Notice the numerous events located west of 235°E along the Mendocino fault. The occurence of events in this region is not unusal as relative motion between the Gorda and Pacific plates is predominately accomodated as right-lateral strike-slip along the Mendocino fault [Bolt et al., 1968; Wilson, 1986; McPherson, 1989; Smith et al., 1993]. The significance of these events in the location procedure stems from the fact that the data used in this study consists

only of events that are archived in the earthquake catalog of the NCSN to have occured **east** of 235°E. It may be argued that the new locations are artificial due to poor hypocentral control for events west of 235°E. However, most of these events include recorded S-phases which effectively improve location control for events outside the network. Furthermore, the majority of these earthquakes occured following the 1 September, 1994, M=6.7 earthquake (234.2°E, 40.4°N) and can be classified as aftershocks as well. It is therefore concluded that these locations are real and reflect the effectiveness of the station array's azimuthal coverage and the inclusion of S phases.

3.3.2 The Wadati-Benioff zone

Seismicity within the quadrant to the northeast of Cape Mendocino (east of 235.8°E, north of 40.3°N) can be identified to be within the Wadati-Benioff zone of the subducting Gorda plate. The distribution of events is broad and diffuse, yet deepens to the east (Figure 3.3). Focal mechanisms in this region are expected to reveal either shallow-dipping thrust events associated with the interaction of the subducting and overriding plates or normal events indicative of internal deformation of the subducting slab. For the majority of events to the northeast of Cape Mendocino, *McPherson* [1989] determined north-south striking, normal mechanisms with the directions of least-principle stress (T-axis) parallel to the downdip of the slab. This suggests that a negative buoyancy force exists within the slab, causing downdip ex-

tension as it is "pulled" into the asthenosphere. Similar observations are made further to the north in the Cascadia subduction zone [Taber and Smith, 1984; Weaver and Michaelson, 1985]. Only a few reverse mechanisms within the east-dipping Wadati-Benioff zone have been detected and may be interpreted as small events related to subduction. The absence of any larger thrust events in this region may either point towards aseismic slip or a strongly coupled interface between the Gorda slab and the overriding North America plate.

The southern boundary of the Wadati-Benioff zone is defined by cessation of seismicity along a trend striking approximately E10°S (Figure 3.3). Interestingly, the Gorda plate also experiences a southward dip in seismic activity along this trend. Verdonck and Zandt [1994] observe this southward flexure in the results of their travel time tomography and conclude that the correlation between seismicity and velocity structure is the best indicator of the top of the Gorda plate. The truncated Wadati-Benioff seismicity, also observed by McPherson [1989], clearly mismatches the southern edge of the Gorda plate as proposed by Jachens and Griscom [1983] to trend 120°N (Figure 3.3). The only events to the south of the Wadati-Benioff truncation is a cluster of events labeled "GF" in Figure 3.3. The hypocentral depth range for these events lies between 10 Km and 30 Km, which makes it impossible to associate them with the surface expression of the Garberville fault alone. Interpretation of these events based on plate geometries poses certain problems: if the southern edge of the Gorda plate were to be defined by the truncation in Wadati-Benioff seismicity, the

"Garberville swarm" [McPherson, 1989] could be either explained as crustal thickening or upwelling of asthenospheric material filling the slab window as the north American plate is no longer underlain by the Gorda plate. In contrast, a southern Gorda edge, as suggested by Jachens and Griscom, would locate the area of mantle upwelling further south and have these events occur in both the Gorda and North American plates. Another interpretation is given by Verdonck and Zandt who interpret the gravity anomaly along the Jachens and Griscom line to represent the northeast edge of the Pacific plate underthrusting North America. They suggest that low upper crustal velocities underlain by normal upper mantle velocities determined from teleseismic travel time inversions [Benz et al., 1992] to the southwest of the gravity line are inconsistent with a shallow asthenosphere. On the basis of seismicity patterns to the east of Cape Mendocino, this interpretation is favored and it is suggested that the southern edge of the Gorda plate is defined by the truncation in Wadati-Benioff seismicity.

3.3.3 Seismicity at the Triple Junction

A more detailed investigation of seismicity at the Mendocino triple junction reveals evidence for a distinct plate boundary between the Pacific and Gorda plates. Figure 3.4 shows a magnified view of the seismicity at the triple junction. Besides the previously noticed area of greatest intensity offshore Cape Mendocino, the area to the south of it is noteworthy for its inactivity. With the exception of a few events, the

transition from intense to absent seismicity occurs abruptly along an east-southeast trend. The area to the south of this trend and its westward extension, the Mendocino fault, is occupied by the Pacific plate. The absence of any significant activity within the Pacific plate is in accordance with rigid plate theory. Seismicity concentrates along its boundary to the Gorda plate, which is much younger in age. The age difference between these two plates causes the Pacific plate to act like a "buttress" [Smith et al., 1993], as it is much colder, thicker and, thus, stronger.

The cessation of seismicity along this east-southeast trend follows the Mattole Canyon fault. Seismic profile studies by Silver [1971] and Clarke [1992] map the Mattole Canyon to lie at the base of a prominent, northfacing escarpment. It branches off the east-west trending Mendocino fault near 235°E to a more southerly trend and projects onshore just south of Punta Gorda and the Mattole River (Figure 3.4). The seismicity, shallow as well as deep, concentrates to the north of Mattole Canyon fault and tapers off when intersecting the coastline at about 235.7°E. This intense concentration of seismicity will be further investigated in terms of focal mechanisms and cross-sections, but there is strong evidence that the trend in seismicity defines a separation between the rigid Pacific plate to the south and the internally deforming Gorda plate to the north.

A cluster of events with focal depths between 5 Km and 15 Km is located in the onshore extension of the Mattole Canyon seismicity, yet clearly separated from the trend offshore (Fig. 3.4). Although it is tempting to interpret these events as a

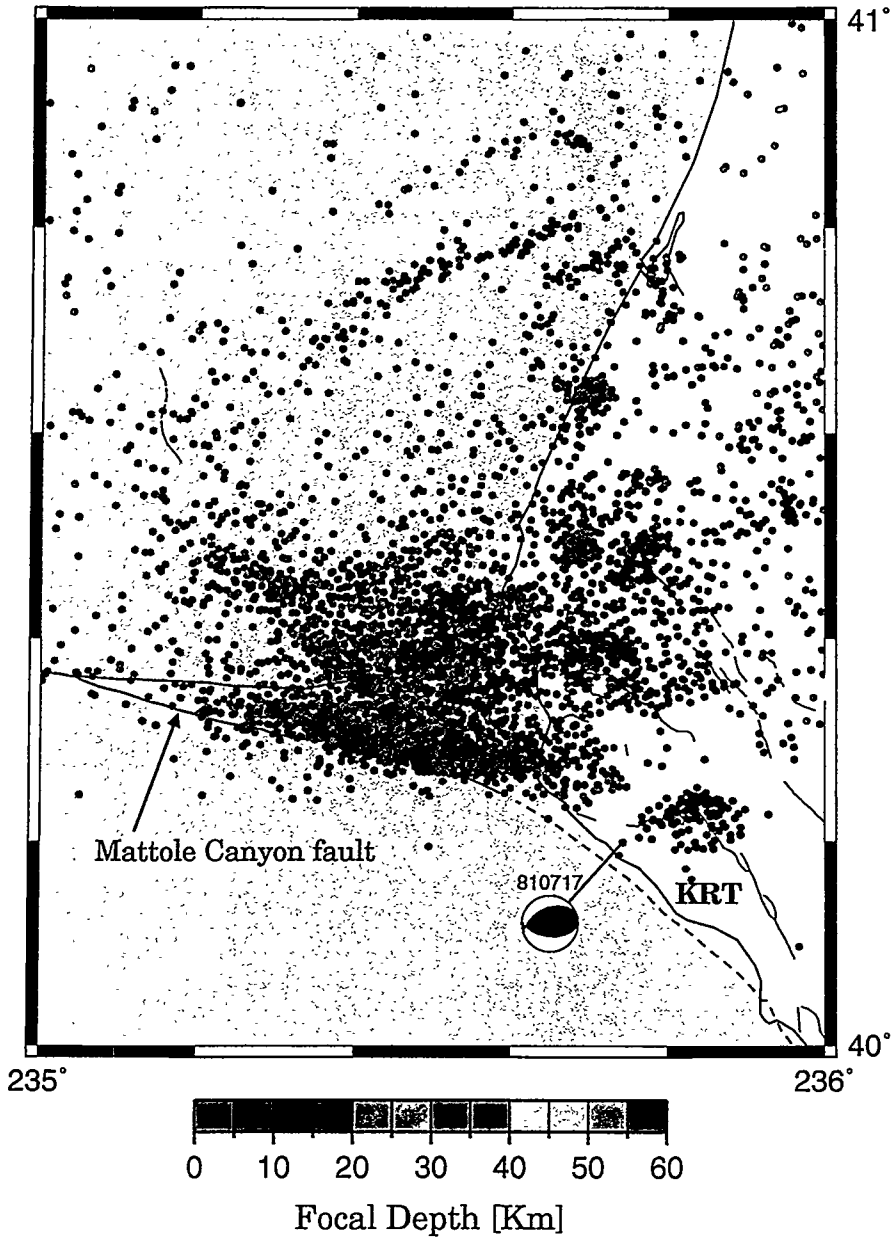

Figure 3.4: Magnified view of seismicity for the region shown by the box in Figure 3.3. Focal mechanism is for the 17 July, 1981 earthquake. KRT, King Range Terrane.

landward extension of seismicity along the Mattole Canyon fault, they are associated with the King Range terrane. This is the westernmost terrane of the coastal belt, containing the youngest accreted rocks of the Franciscan Complex [McLaughlin et al., 1994], and reaching elevations of more than 1200 m within a few kilometers of the coast. In a detailed study of the tectonostratigraphic terranes in the vicinity of the Mendocino triple junction, McLaughlin et al. [1994] suggest that the King Range terrane is a block that accreted to the Pacific plate 14 Ma ago and subsequently obducted onto the North American plate. Tectonic uplift rates for the King Range terrane are reported to be of 1 to 4 mm/yr since 120 Ka and indicate northeast-southwest compression.

The observed seismicity at the northeast side of the King Range terrane is interpreted as thrusting in response to NE-SW compression. Seismicity occurs mainly along the Cooskie shear zone and the King Range thrust zone to the north and east of the terrane, respectively (see Figure 1.2). Cross-sections of the seismicity (Figure 3.12e) indicate a south-west dipping depth distribution in agreement with the expected southside-up thrusting. The only focal mechanism for events within the King Range cluster is from a July 7, 1981, M=4.5 earthquake that was located at the southwest end of activity. The event's reverse mechanism (Figure 3.4) supports the interpretation of thrusting motion. Therefore, the seismic activity at the northern boundary of the King Range terrane is not directly related to the trend in seismicity along the Mattole Canyon fault.

3.3.4 Reference Earthquakes

Thus far the analysis of seismicity has focused on events in the proximity of the Mendocino triple junction. However, the investigation is now focused on the area of highest intensity near Cape Mendocino. It was shown in Figures 3.3 and 3.4 that 24 years of seismic activity produced the previously noted cloud near Cape Mendocino. The following analysis focuses on individual "reference" events and their aftershock sequences with the intention to resolve any pattern and ultimately plate boundaries from this cloud of seismicity.

Several "reference" events that refine the mode of internal deformation of the Gorda plate and the seismicity along the Mattole Canyon fault are shown in Figure 3.5. The purpose of plotting these events on several maps is to demonstrate a spatial correlation between them. Figure 3.5a displays the aftershock sequence of the January 22, 1997, M=5.6 earthquake near Mattole Canyon. Focal mechanisms determined for the mainshock and its January 26, 1997 M=4.0 aftershock indicate near-vertical strike-slip, whereas a M=4.3 aftershock within an hour of the mainshock suggests predominately reverse with a component of strike-slip motion. Cross-sections (not shown) through the mainshock across the rupture plane reveal a sharp cut-off in seismicity to the southwest of Mattole Canyon, while a section parallel to the plane shows an east-dipping trend in hypocentral depths. Based on these observations, this event is interpreted as an interplate earthquake on the boundary between the Pacific and Gorda plates.

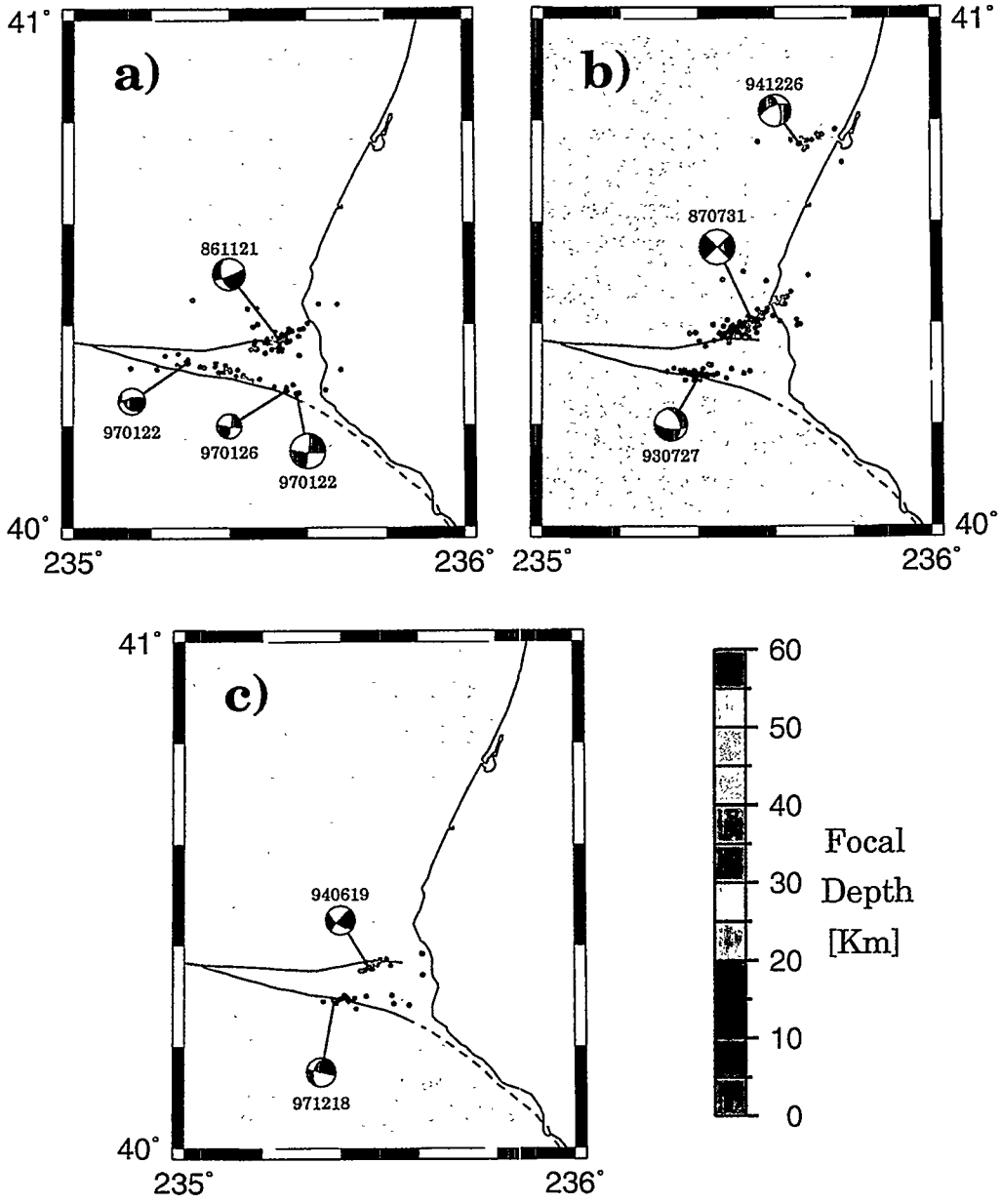

Figure 3.5: Map showing the location of "reference" earthquakes. Focal mechanisms show lower hemisphere projections, with the compressional quadrant shaded. Size of each "beach-ball" is proportional to magnitude. The date of the earthquake is given by the number above or below the focal mechanism [yymmdd].

Several moderate-sized earthquakes offshore near Cape Mendocino are classified as intraplate events of the Gorda plate. The November 21, 1986 M=5.1 (Figure 3.5a), the July 31, 1987 M=5.6 (Figure 3.5b) and the June 19, 1994 M=4.7 (Figure 3.5c) earthquakes occured on northeast-southwest trending planes within a few kilometers of each other. The June 7, 1975 magnitude 5.2 Ferndale earthquake and its aftershock sequence [Smith, 1975] occured a few kilometers north of these events on a similar northeast striking fault plane. The focal mechanisms for the mainshocks of these sequences show mainly strike-slip motion and it is concluded that internal deformation of the Gorda plate is expressed in form of left-lateral strike-slip on northeast trending faults. The December 26, 1995, M=4.9 earthquake offshore of Humboldt Bay (Figure 3.5b) supports this interpretation.

The analysis of "reference" events also includes two shallow events along the Mattole Canyon fault. The July 27, 1993, M=3.9 (Figure 3.5b) and the December 18, 1997, M=4.4 (Figure 3.5c) events and their aftershocks are confined to depths between 5 and 10 Km. As is the case of the deep event (1-22-1997), the aftershocks align near vertically and define a sharp cut-off along the Mattole Canyon fault. It is interesting to investigate whether the shallow activity along the Mattole Canyon fault corresponds to interplate activity and defines a plate boundary.

3.3.5 The 1991 Honeydew and 1992 Cape Mendocino Thrust Earthquakes

The August 17, 1991, M=6.2 Honeydew and the April 25, 1992, M=7.1 Cape Mendocino earthquakes are the first recorded, large thrust events associated with subduction along the Cascadia megathrust. These events are the largest to occur onshore near the Mendocino triple junction in recorded history, and caused considerable damage in the towns of Petrolia and Honeydew [Velasco et al., 1994; McPherson and Dengler, 1992]. Both events are considered to have relieved strain due to Gorda-North American plate convergence [Oppenheimer et al., 1993]. Furthermore, the 1992 mainshock triggered two M=6.6 aftershocks that are located within the Gorda plate. The events' similarities as well as their differences have great significance to the investigation of seismotectonics at the triple junction.

The 1991 Honeydew earthquake is interpreted to have occured on a shallow, east-dipping thrust fault. The event is located at a depth of 12.4 Km about 4 Km east of Punta Gorda. Figure 3.6a shows the location of the mainshock and seismic activity during a 14-day period following the mainshock, as well as locations and focal mechanisms of the mainshock determined by other investigators (e.g. Dziewonski et al. [1992], Oppenheimer and Magee [1991]). The displayed focal mechanisms indicate some uncertainty in the amount of fault dip. Furthermore, the question which of the two possible fault planes ruptured during the mainshock has been a matter of debate. McPherson and Dengler [1992] report a 6 Km northwest trend of extensional cracks

and the area of highest intensities to the southeast of the mainshock. They interpret their observations as reverse slip on the focal plane that dips steeply to the southwest. Yet, their interpretation does not take into account the seismic aftershock activity extending west as far as 15 Km of the mainshock.

Cross-sections agree with an interpretation of an east-dipping thrust fault. Figure 3.6b shows the eastward dip in the distribution of seismicity, with the location of the mainshock at the zone's downdip termination. A cross-section through the more intense cluster at the sequence's up-dip termination (Figure 3.6c) reveals a previously recognized sharp cut-off in seismicity towards the southwest that can also be observed in the map view of Figure 3.6a. Based on these observations, the following is proposed: the Honeydew earthquake occured on a relatively shallow, east dipping thrust fault; this low-angle thrust fault is believed to be within the modern subduction complex of the North America plate and not along the Gorda-North America interface, since this is believed to be around 18-20 Km deep (Verdonck and Zandt [1994] propose this to be the case for the 1992 Cape Mendocino earthquake); the sharp cut-off in seismicity along Mattole Canyon corresponds to the North America plate boundary. This interpretation suggests that the aftershocks and earthquakes are confined to the North American plate due to stress changes imposed by the mainshock and, in general, terminate when reaching the plate boundary.

Similar focal mechanisms and the close proximity of the hypocenters have led some investigators to consider the 1991 Honeydew earthquake to be a preshock to the 1992

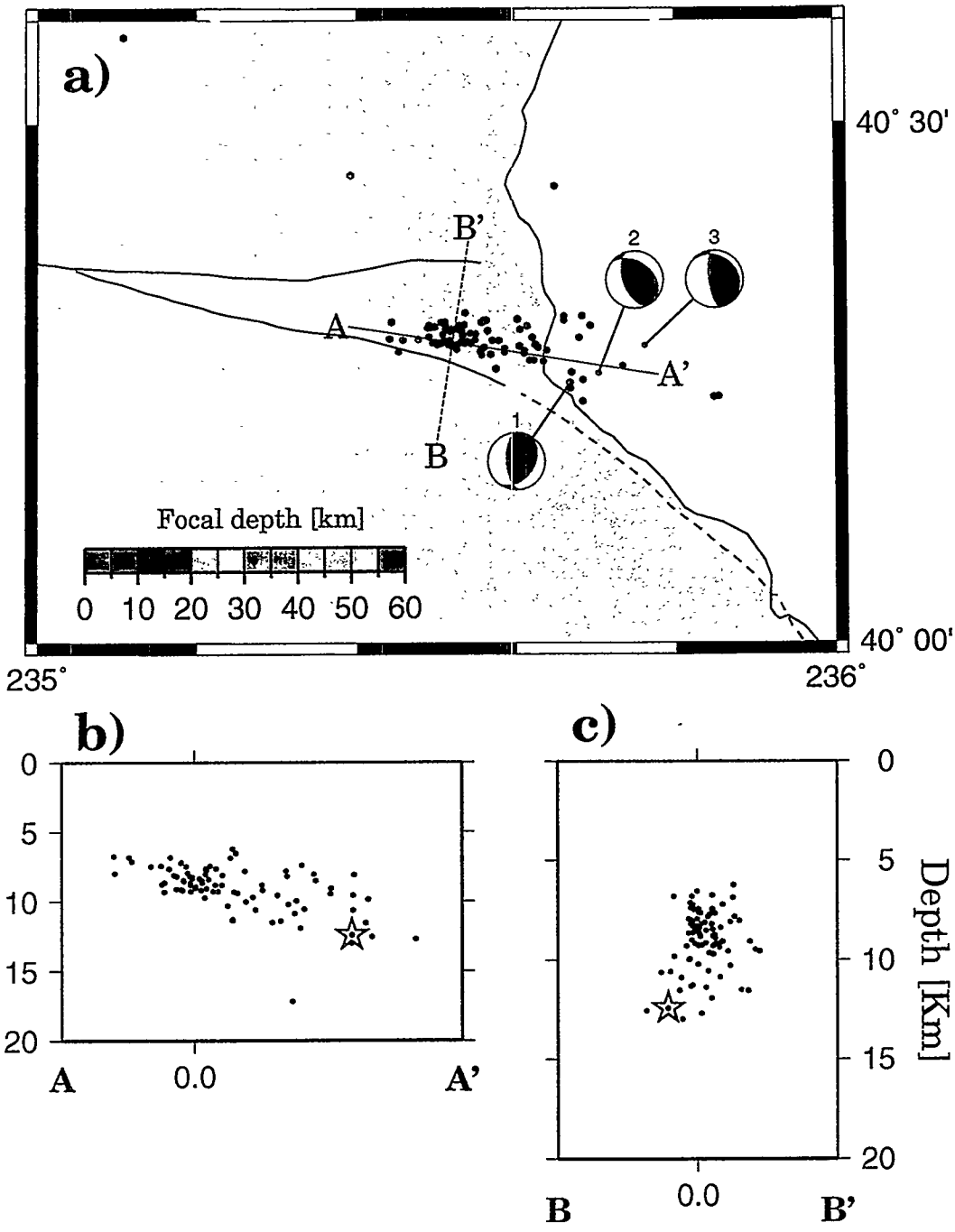

Figure 3.6: The August 17, 1991, Honeydew earthquake. (a) Map view of epicenters for a 2-week period following the mainshock and focal mechanisms for the mainshock by various investigators: (1) location and focal mechanism (after Dreger [1998]) of this study, (2) after Dziewonski et al. [1992], (3) after Oppenheimer and Magee [1991]. (b) Cross-section along the line connecting A and A' in (a). (c) Cross-section along BB'. Red stars show the location of the mainshock in the cross-sections.

Cape Mendocino earthquake. The 1992 event is located approximately 6 Km north of the Honeydew epicenter at a depth of 15.5 Km, although Oppenheimer et al. [1993] report a slightly shallower depth of 10.6 Km. Figure 3.7 shows the seismic activity following the mainshock for a two-month period and solutions for the main- and two large aftershocks by various investigators. The focal mechanism of the mainshock is well constrained this time and indicates slip on a shallow, northeast dipping thrust fault. The earthquake caused considerable coseismic deformation: Murray et al. [1996] report maximum displacements of 0.4 m horizontally and 1.5 m vertically along the coastline. Similar coseismic uplifts are assumed to have occured a minimum of four times between 600 and 7000 years ago [Merrits, 1996], suggesting that this may be a characteristic event for the southern end of the Cascadia subduction zone.

The rupture of the mainshock propagated westward (updip) and is modelled to parallel the direction of convergence between the Gorda and North American plates. Murray at al. [1996] report 3.5 m of thrust dip-slip motion in the direction of 250°N based on modeling the coseismic deformation. However, the location of the mainshock hypocenter (depth=15.5 Km) at the downdip end of the fault implies that it did not rupture the Gorda-North American interface directly, but was a blind thrust fault within the overriding North American plate. Seismicity within the Gorda plate concentrates itself at depths greater than 18-20 Km at the triple junction (chapter 3.3.4), well below the mainshock depth. Verdonck and Zandt [1994] come to the same conclusion that crustal velocities at depths of 15 Km are too slow to be associated with

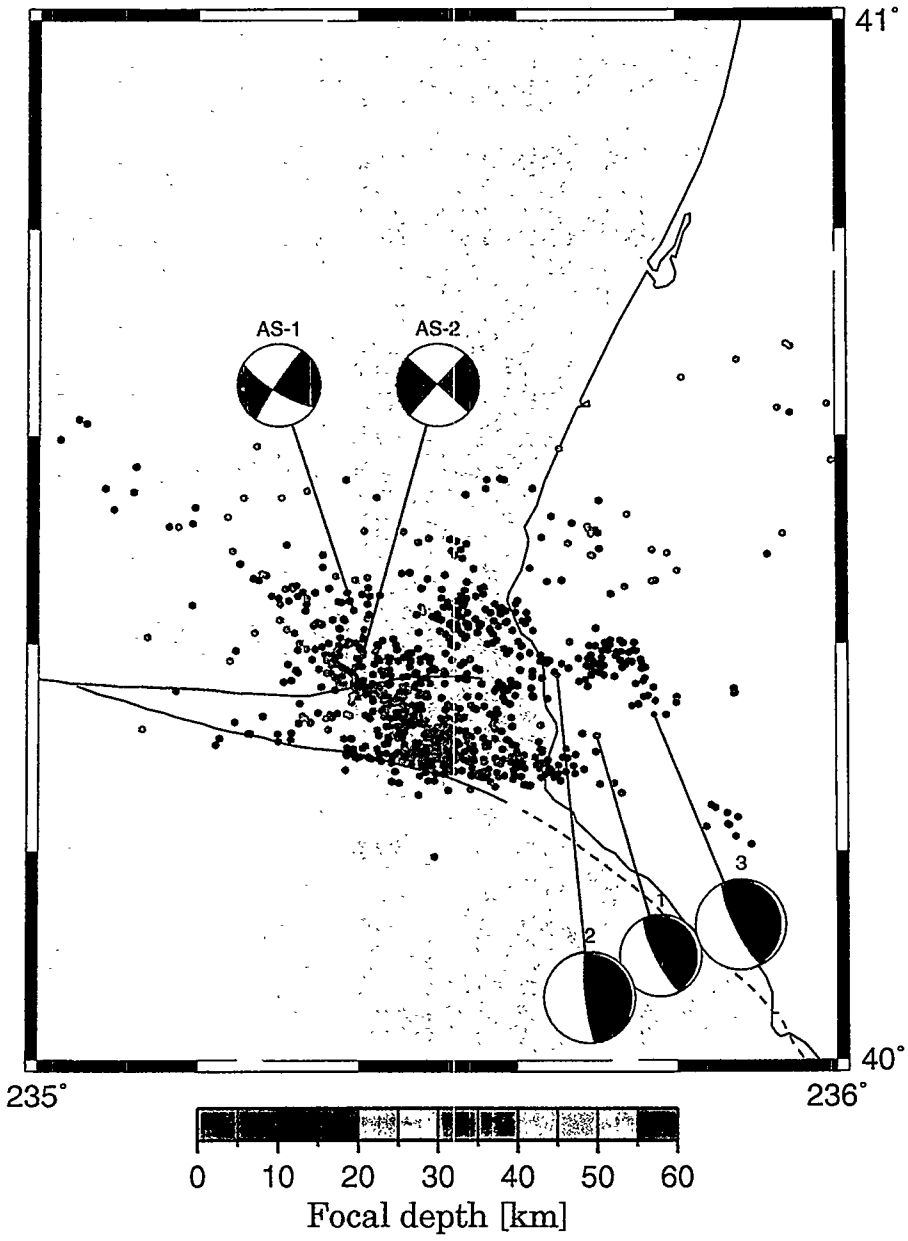

Figure 3.7: The April 25, 1992 Cape Mendocino earthquake. Map shows epicenters of earthquakes during the two months following the mainshock. Location and focal mechanism for the mainshock are: (1) this study (mechanism after Dreger [1998]), (2) after Dziewonski et al. [1993], (3) after Oppenheimer et al. [1993]. Also shown are the focal mechanisms for two M=6.6 aftershocks.

oceanic crust. If this is the case, the aftershock seismicity on the shallow dipping rupture plane should be confined to the North American plate and define another sharp cut-off at the boundary to the Pacific plate.

Shallow seismicity after the Cape Mendocino earthquake concentrates along two west-northwest oriented lineations but does not show any planar structure associated with a dipping thrust fault. Figure 3.8a shows the epicenters for earthquakes located above 16 Km depth. With the mainshock at the lower limit and considering rupture updip, the displayed seismicity is considered to have occured in the North American plate. Also plotted in Figure 3.8a is the slip vector and the surface projection of the SE-dipping thrust fault that best-fit the observed geodetic coseismic displacements (after Murray et al. [1996]). The two trends in seismicity are located near the southern and northern edges of the inferred fault plane. The southern edge seismicity coincides with the previously recognized seismicity along Mattole Canyon and becomes denser towards its western end near 235.4°E. Cross-section AA' (Figure 3.8c), which is perpendicular to the seismic trend, shows the vertical cut-off in seismicity above 16 Km. The mainshock focal mechanism, the geometry of the rupture plane and the direction of slip indicate that these events are induced by a stress-field perturbation in the compressional quadrant of the mainshock. In this case, the area of dense epicenters at the western end of this zone would have experienced the largest stress changes. Furthermore, the vertical cut-off to the southwest supports the interpretation of the North America-Pacific plate boundary: any stress perturbation

acting on the northern Pacific plate is not sufficient to overcome the much greater strength of that plate and seismicity is confined to the North American plate. Seismicity near the fault plane's inferred northern edge is more diffuse and is interpreted to be associated with the contractional forearc region of the subduction zone and/or onshore faults such as the Russ and Capetown faults (see Figure 1.2) as mapped by Kelsey and Carver [1988].

The occurence of two M=6.6 aftershocks in the Gorda plate within 24 hours of the mainshock may be indicative of strong coupling between the North American and Gorda plates. The focal depths of 21.3 Km for the first and 23.6 Km for the second aftershock clearly identify these events as occuring in the Gorda plate (Figure 3.8b). Although the strike-slip focal mechanisms are consistent with internal Gorda plate deformation on left-lateral, northeast striking fault planes (chapter 3.3.4), there is evidence that they ruptured the conjugate planes striking northwest-southeast. Oppenheimer et al. [1993] report strong variations in amplitudes of broadband velocity records with a maximum at 130°N for the second aftershock. The variations are interpreted as directivity effects associated with rupture on the southeast striking nodal plane. Unequivocal identification of the first aftershock fault plane has not been possible so far, mainly due to the lack of any directivity effects and the paucity of aftershocks. However, Velasco et al. [1994] prefer rupture on the conjugate plane striking to the northeast.

Aftershock seismicity within the Gorda plate is in agreement with rupture on a

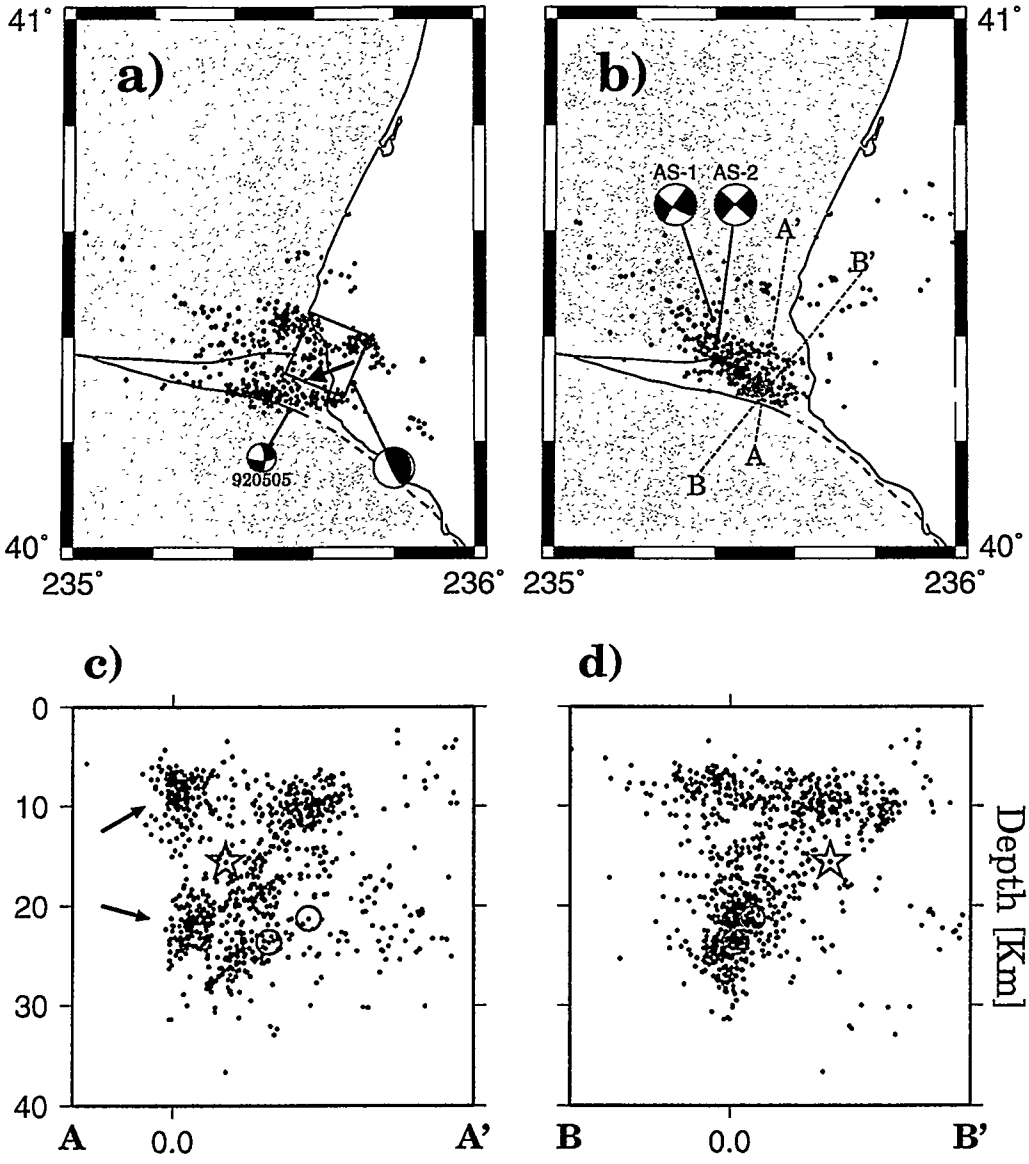

Figure 3.8: Partition of seismicity following the 25 April, 1992 Cape Mendocino earthquake. (a) Map of epicenters with focal depths less than 16 Km. Focal mechanisms are for the 25 April mainshock and an aftershock on 5 May. Solid rectangle shows the surface projection of the ruptured thrust fault with red arrow indicating the uniform slip direction (after Murray et al. [1996]. (b) Epicenters of earthquakes with focal depths greater than 16 Km. (c) and (d) Cross-sections along lines as indicated in (b). Red star denotes location of the mainshock, red circles locations of the two M=6.6 aftershocks. Note the near vertical truncation of hypocenters as indicated by the two red arrows in (c).

northwest-southeast fault plane. Figure 3.8b shows a linear trend of deep seismicity in correspondence to a southeast rupture. However, the absence of any lineations in the northeasterly direction that may be associated with the first aftershock adds to the ambiguity in fault planes for this event. Another feature that can be observed in the distribution of Gorda plate aftershocks is the area just to the north of Mattole Canyon, which shows rather diffuse seismicity, but another sharp truncation between 18 Km and 25 km depth. In cross-sectional view (Figure 3.8c), this termination projects vertically from the truncation in shallow seismicity recognized earlier. At this point it must be stressed that these abrupt terminations of seismicity are not artificial: if there had been activity to the southwest of this lineation, it would have been detected by the seismic network. The cross-section of Figure 3.8d (BB') shows the vertical distribution of aftershocks in the Gorda plate. The distribution is rather diffuse and does not define a distinct vertical rupture plane associated with the two strike-slip aftershocks.

3.3.6 Bimodal Depth Distribution of the Seismicity

On the basis of the analysis of the 1992 Cape Mendodino earthquake, it is found useful to partition the seismicity at the Mendocino triple junction in depth intervals. The cross-sections for the 1992 Cape Mendocino earthquake (Figures 3.8c and d) indicate that activity concentrates above and below the mainshock focal depth. This criterium is applied to divide the seismicity displayed in Figure 3.4 into events that

are located in the upper 16 Km (Figure 3.9) and those events below this depth (Figure 3.10). However, this partitioning does not represent a discrete plate boundary between the North American and Gorda plate, but rather a general division between intraplate seismicity of each plate.

Seismicity between 1974 and 1998 at shallow depth occured in several northwest oriented trends of which the most prominent aligns with Mattole Canyon. Figure 3.9 is a summary of earthquake activity in the upper 16 km, presumably within the North America plate. The previously recognized activity along Mattole Canyon displays a geometry that is wedge-like, thinning to the west and extending to about 235.3°E. The activity's eastern termination is more diffuse and extends to ca. 235.7°E. Further east of this activity map the epicenters that are associated with the King Range terrane, as discussed in chapter 3.3.3. The west-northwest oriented trend in seismicity near Cape Mendocino was noted earlier as a zone that experienced activity following the 1992 Cape Mendocino earthquake. The remaining seismicity maps rather diffusely and may be related to mapped faults (i.e. the Russ and Capetown faults [Kelsey and Carver, 1988]), although Smith et al. [1993] do not see a clear seismic expression of these faults. McPherson [McPherson, 1989] found for the majority of shallow events within the North American plate northwest striking, reverse mechanisms, indicative of forearc contraction of the Cascadia subduction zone.

Figure 3.10 shows the epicenters of events with hypocentral depths greater than 16 km. Additionally, focal mechanisms are plotted for a number of events in order to

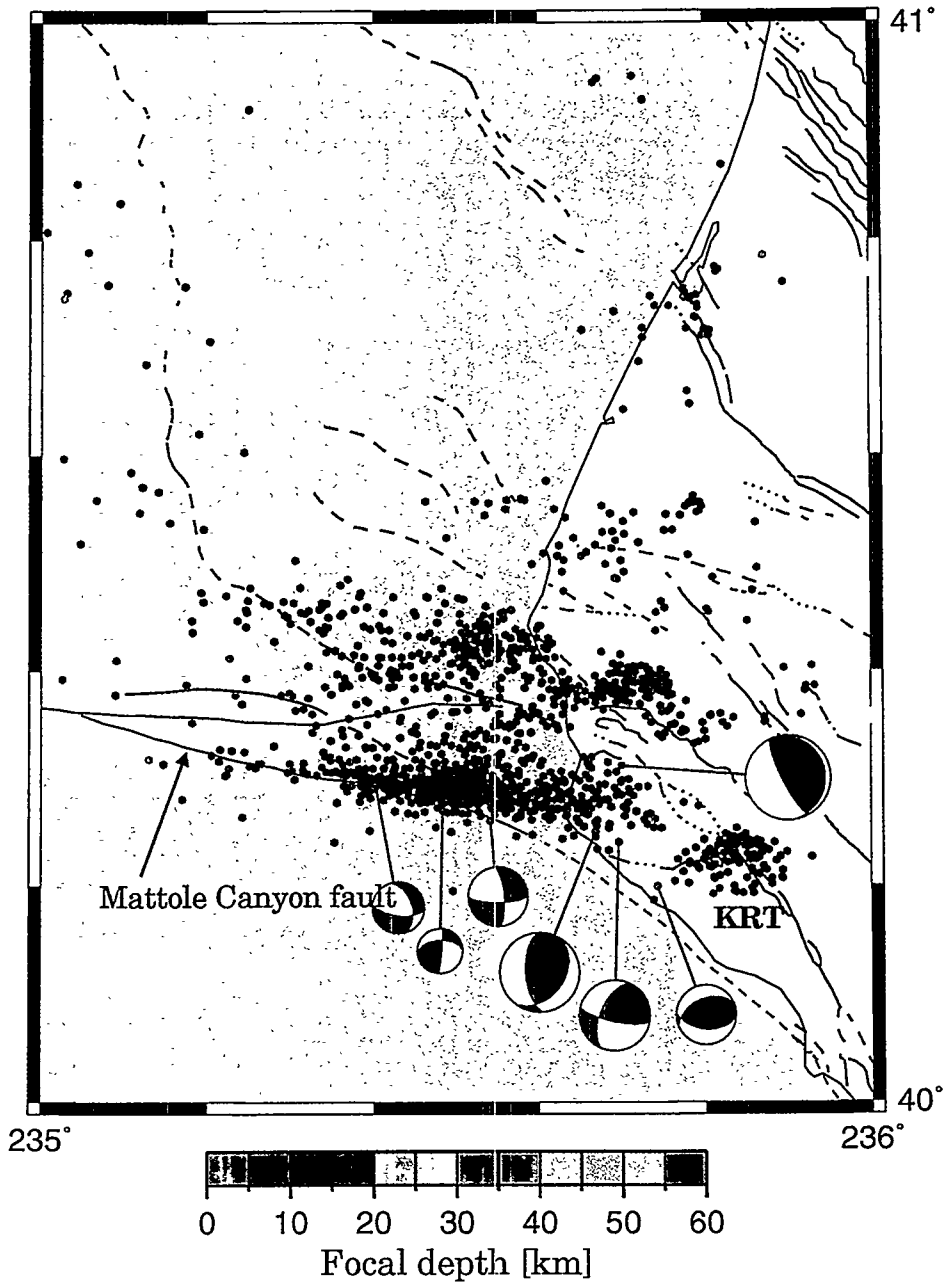

Figure 3.9: A summary of seismicity between 1974 and October 1998 for events with hypocentral depth less than 16 Km. Focal mechanisms show lower hemisphere projections. KRT-King Range Terrane.

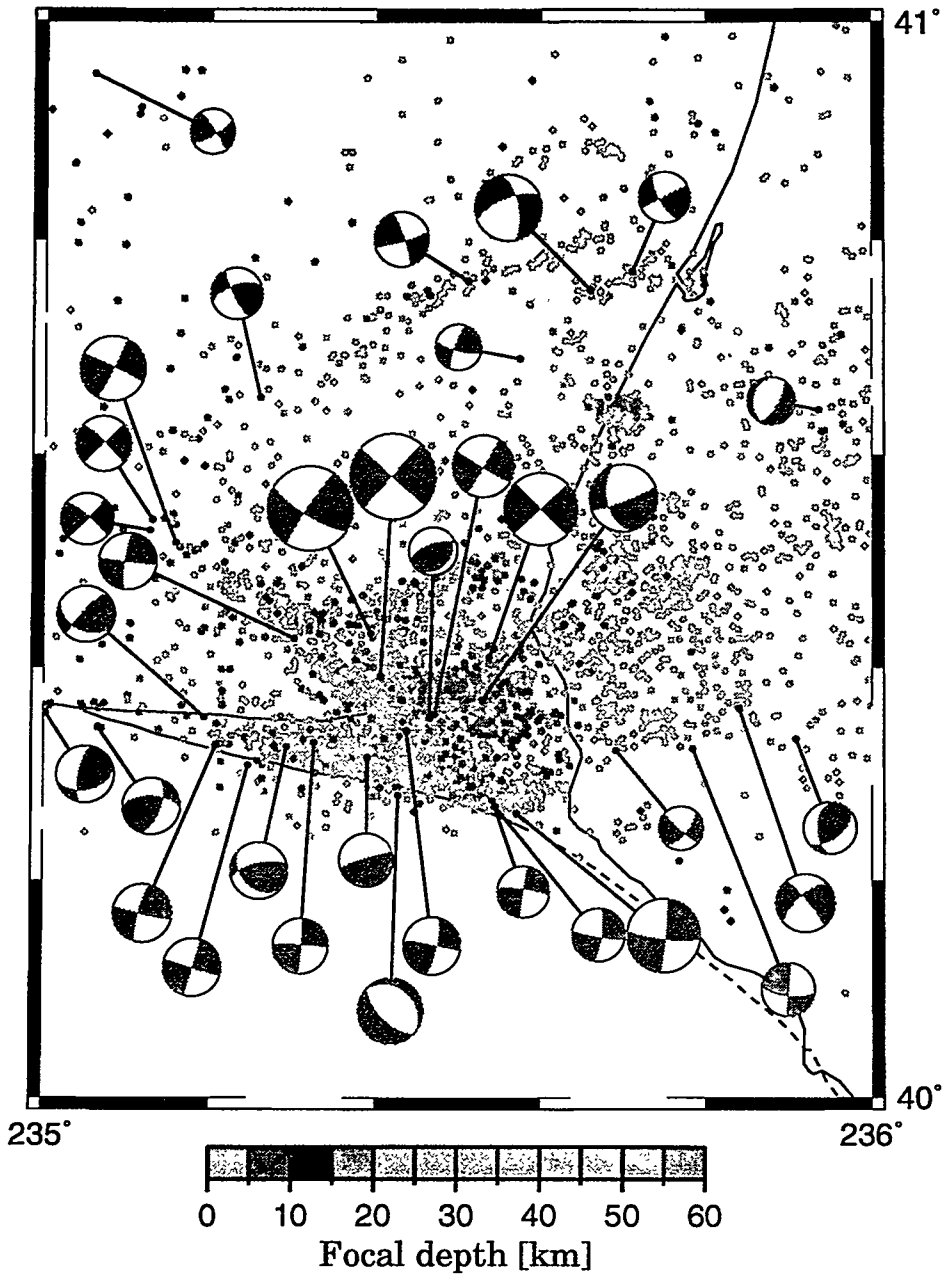

Figure 3.10: Map view of epicentral locations for earthquakes that are located deeper than 16 Km. Focal mechanisms show lower hemisphere projections.

illustrate the conformity with a single north-south stress orientation. The mechanisms agree with the earlier interpretations that internal deformation of the Gorda plate is accomodated along either northeast-southwest or northwest-southeast trending fault planes. The analysis of the reference events (chapter 3.3.4) and the aftershocks of the 1992 Cape Mendocino earthquake suggested that slip occurs on either nodal plane, however, several lineations of epicenters in northeasterly direction may be interpreted as mainly rupture on that nodal plane. Events that are located along Mattole Canyon, presumably at the Gorda-Pacific plate boundary, show a slighly rotated focal mechanisms, in agreement with the trend of highest activity. Notice also how seismicity along Mattole Canyon terminates at the coastline near Punta Gorda (235.6°E).

3.3.7 Cross-sections of Hypocenter Distributions

To further investigate the distribution of hypocenters with depth, the seismicity shown in Figures 3.9 and 3.10 is displayed in a series of cross-sections. The strike and length of each of the seven constructed cross-sections are shown in Figure 3.11a.

In east-west sections, which parallel the strike of the Mattole Canyon fault, a zone of seismic quiescence separates two eastward dipping zones of intense activity. A slice through the seismicity along Mattole Canyon (cross-section AA', Figure 3.11b) shows a separation of approximately 6 Km between the shallow and deep seismic trends. The shallow activity appears wedge-shaped and thinning towards its western end,

where the majority of earthquakes are located. To the east, a seismic gap of ca. 5 Km separates this elongated trend from the cluster that was previously associated with thrusting motion of the King Range terrane. Termination of seismicity within the deeper trend occurs near the coastline at Punta Gorda, in agreement with the conclusion drawn from map view.

A second east-west section crosses the coastline near Cape Mendocino and demonstrates the extent of intraplate deformation of the east-dipping Gorda plate (cross-section BB', Figure 3.11c). Hypocenters are located at depth in an approximately 12-15 Km wide zone that displays a shallow east-dipping trend. The separation to the directly overlying seismicity west of Cape Mendocino is not as pronounced as in the section farther to the south, and isolated earthquakes are located in between the two zones. However, a void of earthquakes to the east of Cape Mendocino can be observed between a depths of 12 and 20 Km and initiation of seismicity occurs sharply along a shallow dipping plane near 20 Km depth. If this initiation of seismicity defines the depth to the top of the Gorda plate near Cape Mendocino, the question arises why earthquakes further west do not project within this planar structure? The likely reason is that uncertainties in hypocentral depth estimates increase for events outside the land-based seismic network, resulting in a more scattered distribution of hypocenters in depth. However, the concentration of earthquakes along the top of this band of seismicity clearly displays an eastward dip and is interpreted to define the top of the oceanic crust of the Gorda plate.

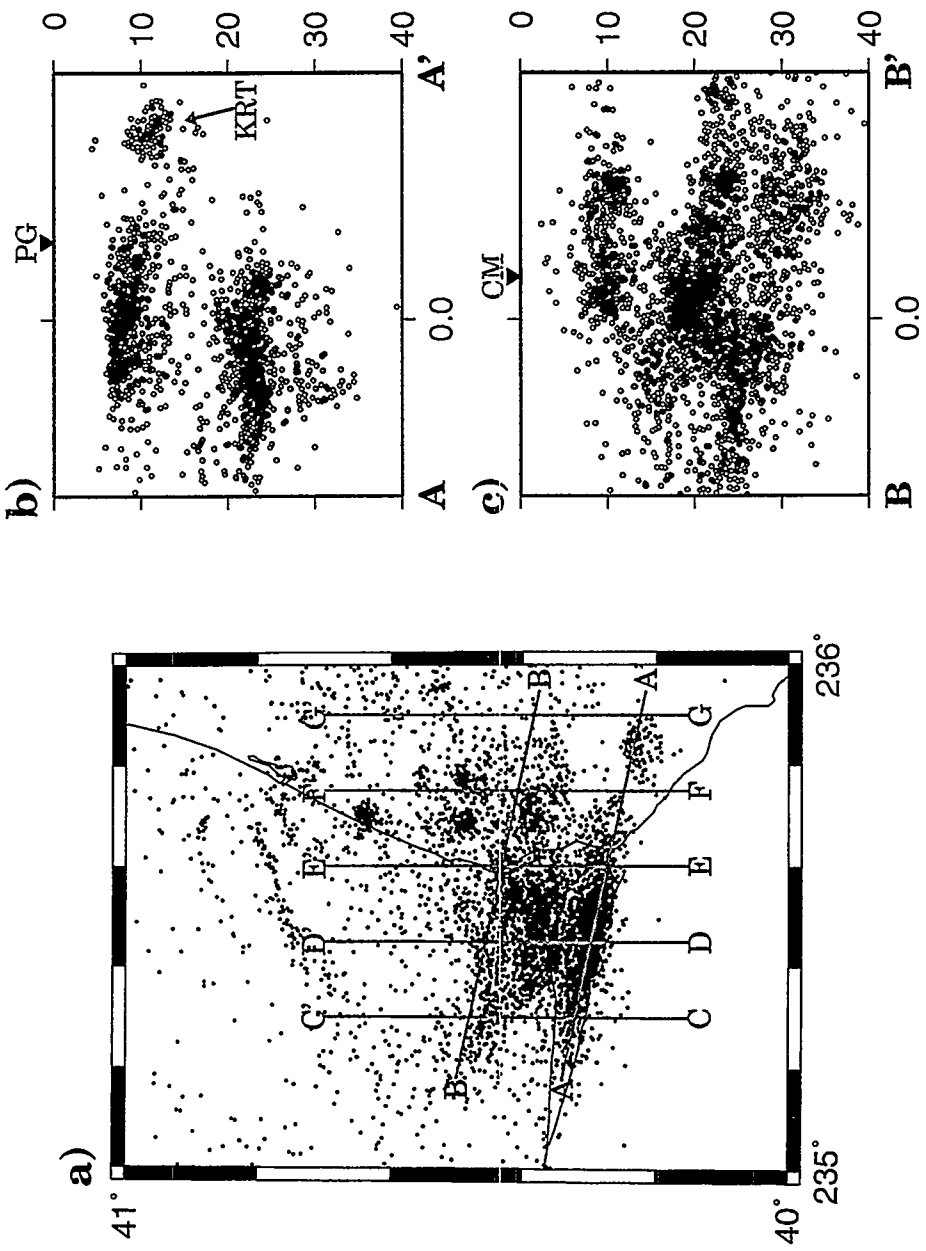

Figure 3.11: East-west cross-sections of seismicity at the Mendocino triple junction. (a) Location of sections AA' through GG' that are displayed in (b) and (c) and Figure 3.12. (b) East-west seismic section along AA', showing the distribution of seismicity along the strike of Mattole Canyon. (b) Seismicity projected on the section connecting points B and B' in (a). PG, Punta Gorda; CM, Cape Mendocino.

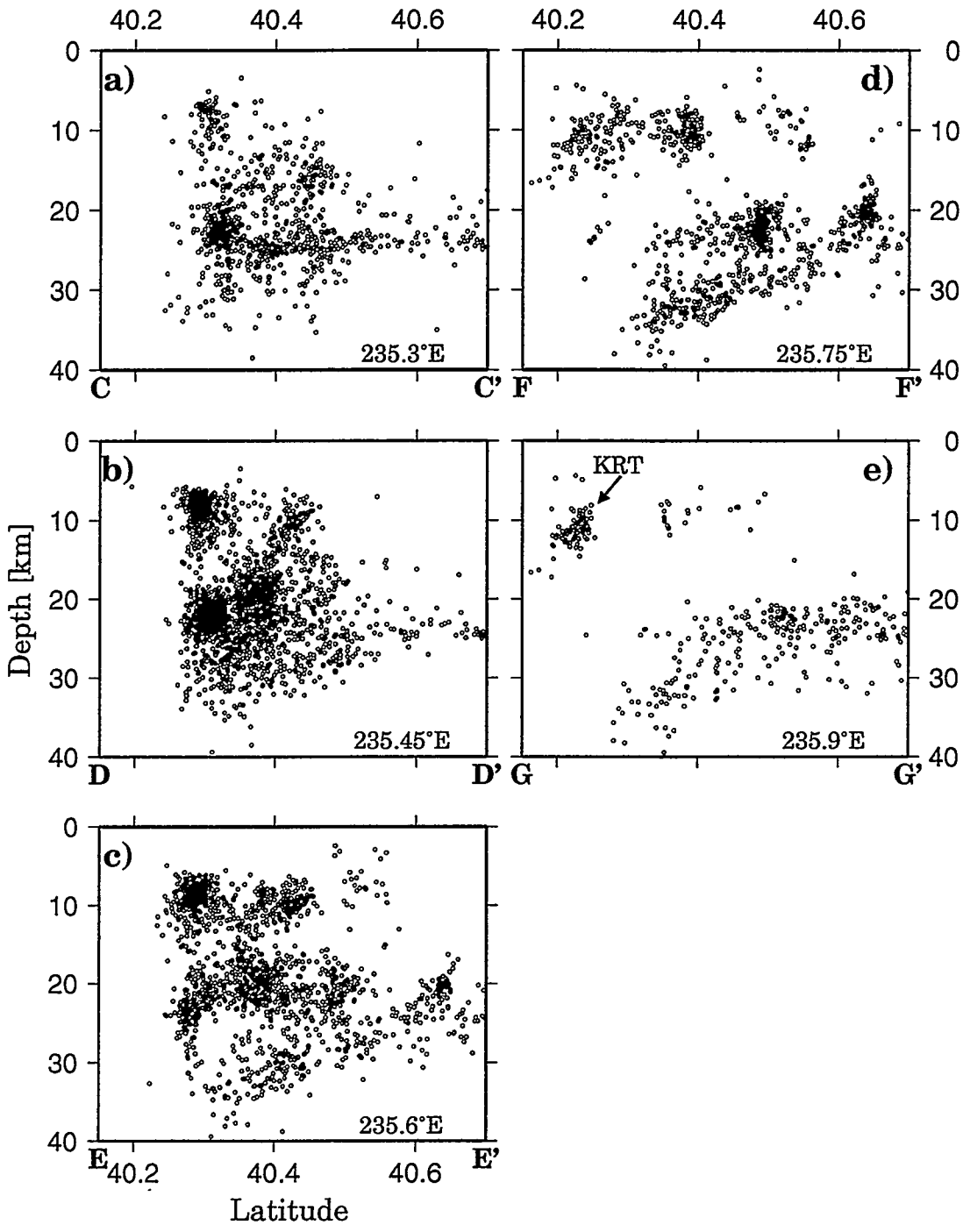

Figure 3.12: A series of north-south seismicity sections. Location and length of each section is given in Figure 3.11a. Each section is centered at the longitude given in the lower right-hand corner and projects the seismicity within a 0.15° bin. KRT: seismicity associated with the King Range terrane.

A series of north-south cross-sections is constructed and completes the analysis of the seismicity distribution. Figure 3.12 shows five north-south seismic sections that traverse the Mendocino triple junction in easterly direction, each covering a 0.15° wide bin. The three westernmost sections (Figures 3.12a-c) clearly illustrate the near vertical cut-off in seismicity along Mattole Canyon. Cross-section DD' (Figure 3.12b) displays the highest concentration of earthquakes along Mattole Canyon, possibly indicating the area of greatest stress within the North American and Gorda plate along their boundary to the Pacific plate. Earthquakes projected onto the two easternmost sections (FF' and GG', Figures 3.12d and e) show the locations of earthquakes within the approximately 10 Km wide zone below 20 Km depth that was noticed in the east-west sections. Notice, however, that these hypocenters also describe a southward bending lineation that is most pronounced in section FF' (Figure 3.12d). This southward dip reaches values of nearly 45° and extends to depths of 40 Km in section FF'. There seems to be a relation between the termination of Gorda-Pacific interplate seismicity along Mattole Canyon near the coastline at Punta Gorda and initiation of activity in this observed southward dipping zone. This change in seismic activity may be explained by stress changes within the Gorda plate. As the plate moves past the obstruction that is created by the northeastern edge of the Pacific plate, internal stress of the Gorda plate is perturbed and is expressed in a change of seismic activity.

Chapter 4

Discussion and Conclusions

4.1 Introduction

In this study relocated hypocenters are used to identify patterns of seismicity and to infer crustal structures at the Mendocino triple junction. The estimation of hypocenter locations has been recognized as a powerful tool at the MTJ due to the intense seismotectonic activity of the region. However, this analysis is limited to seismically active regions. Any area with seismic quiescence does not provide information and requires extrapolation of information.

The data presented in the previous chapter illustrate that a map of the abundant earthquakes in the region contains some diffuse but revealing patterns. A classification of the spatial distribution of earthquakes in terms of inter- and intraplate processes is essential in inferring the crustal structure. The following discussion focuses on

the three-dimensional crustal structure in the triple junction region. An important question in the assessment of seismic hazards for Northern California is the amount of seismic coupling between the subducting Gorda plate and the overriding North America plate. The answer to this question is further complicated by the fact that the Gorda plate undergoes internal deformation, which is a deviation from rigid plate behavior. The results of this study provide some insight into the processes that drive the evolution of the Mendocino triple junction.

4.2 The North American Plate

Deformation in the North American plate at the Mendocino triple junction can be classified into three tectonic regimes. North of Cape Mendocino, deformation within the forearc contractional zone of the Cascadia Subduction zone is expressed as northwest trending thrust faults and associated folds. A zone of lateral translation, expressed by predominately right-lateral coseismic slip, aligns with the Mattole Canyon fault and projects onshore at Punta Gorda. Southeast of Cape Mendocino, a northeastward-directed compressional regime is associated with thrusting motion of the King Range terrane.

Despite geological evidence of Quaternary deformation within the contractional zone of the accretionary wedge, the correlation between seismicity and mapped faults is weak. Kelsey and Carver [1988] refer to a 30 Km wide zone of thrust faults and folds north of Cape Mendocino and around Humboldt Bay as the forearc contraction

of the North American plate. They report a minimum of 7.9 Km northeast-southwest shortening across thrust faults in the region through Quaternary time, although these faults do not show any obvious seismic expressions. First motion results reported by McPherson [1989] agree with a near-horizontal, north-northeast principle compression axis. These observations indicate that deformation in the contractional zone of the North American plate on northwest oriented, northeast dipping reverse faults occurs as a result of plate convergence with the subducting Gorda plate. Furthermore, Kelsey and Carver [1988] argue that the observed amount of shortening within the forearc contractional zone requires strong coupling between the two converging plates.

The scattered distribution of relocated earthquakes in the forearc region of the Cascadia subduction zone is interpreted to reflect the diffuse seismicity on shallow dipping thrust faults. The results of events that are located at depths less than 16 km (Figure 3.9) demonstrate the difficulty of relating seismicity to mapped faults in this region. The previously observed concentration of earthquakes within a west-northwest striking trend near Cape Mendocino maps diffusely at the southern end of the forearc region. Although this seismicity cannot be attributed to a single fault, the trend seems to follow the direction of shear fabric and faults in the region as mapped by Kelsey and Carver [1988]. They argue that thrust faults in the forearc region do not manifest frequent seismicity, and therefore, these faults must release stress in large, infrequent earthquakes. The observation that this region of the forearc contraction zone experienced coseismic deformation following the 1992 Cape Mendocino

earthquake supports their interpretation.

The occurence of the 1991 Honeydew and 1992 Cape Mendocino earthquakes is consistent with an interpretation that convergence of the North America and Gorda plate causes brittle failure on shallow thrust faults in the forearc contractional zone. For both events, focal mechanisms and the distribution of aftershocks indicate that failure occured on blind thrust faults in the accretionary wedge of the subduction zone and not on the subduction interface itself. However, the significance of these events on the definition of plate boundaries at the triple junction lies in the distribution of seismicity induced by the mainshocks. The lack of aftershocks south of the Mattole Canyon fault in the Pacific plate reinforces the interpretation that strain due to Gorda and North America plate convergence was released during these events and the strike of the Mattole Canyon fault defines the Pacific-North America plate boundary.

Seismicity at shallow depths along the Mattole Canyon fault occurs in a zone of right-lateral translation that is interpreted to define the plate boundary between the Pacific and North America plates. Earthquakes within this zone extend west to about 235.4°E (Figure 3.9), display an eastward dip and are located at depths less than 12 Km (Figure 3.11b), too shallow to be associated with the Gorda plate. Focal mechanisms for events within this cluster show predominately right-lateral strike-slip, with components of normal and reverse motion. However, the series of north-south cross-sections (Figure 3.12) does not show any underthrusting motion beneath the Pacific plate, but more of a vertical truncation of seismicity along the strike of Mat-

tole Canyon. The attribution of seismicity along Mattole Canyon as the eastern-most extension of the Mendocino Fracture zone to interplate activity between the North America and Pacific plate implies certain problems with earlier proposals that the Mendocino triple junction currently locates southeast of Cape Mendocino (e.g. McLaughlin et al. [1994]). Based on the results of this study, it is suggested that the Mendocino triple junction is situated offshore, where it has traditionally been located.

The third regime of seismotectonic activity within the North America plate is associated with north-northeast directed thrusting motion along the north and northeast sides of the King Range terrane. McLaughlin et al. [1994] suggest that the King Range terrane is accreted to the northeastern edge of the Pacific plate and is currently being uplifted due to northeast-southwest compression between the North American and Pacific plates. The trace of the San Andreas fault has traditionally been projected offshore from the King Range terrane (Figure 3.9), although it has never been delineated in this region. The only evidence for the San Andreas fault is this region comes from observed surface cracks that were observed near Point Delgada following the 1906 San Francisco earthquake. Thus, the possibility has been considered that the San Andreas fault lies along the east side of the King Range terrane and intersects with the eastward projection of the Mattole Canyon fault to the north of the terrane. Although there is no seismicity evident along the presumed San Andreas fault trace offshore, observations of seismicity are inconclusive as to whether the present day San Andreas fault locates to the east of the King Range terrane. This uncertainty reflects

the complexity in crustal structure at the Mendocino triple junction.

4.3 The Gorda Plate

The distribution of seismicity associated with the Gorda plate can be classified into three types: 1) internal deformation, a deviation from rigid plate models occurs west of 236°E under north-south compression on predominately northeast-southwest striking rupture planes; 2) seismicity along the Mendocino Fracture zone and its southeasterly extension, the Mattole Canyon fault, is interpreted as interplate activity with the Pacific plate; 3) seismicity east of 236°E is located within an southeast dipping Wadati-Benioff zone of the Gorda plate.

The majority of earthquakes at the Mendocino triple junction occur within the Gorda deformation zone. Silver [1971] first suggested that deformation of the oceanic crust occurs on northeast striking, left-lateral faults along in situ zones of weakness that parallel the magnetic anomalies. Several lineations and aftershock sequences have been identfied from the results of relocated hypocenters that support this interpretation. Focal mechanisms for events in this region agree with the inferred north-south direction of maximum compression. The abundance of earthquakes within the Gorda plate near Cape Mendocino (Figure 3.10) suggests that stresses are greatest there.

The observed intraplate seismicity of the Gorda plate induced by a north-south compressional stress regime can be attributed to the convergence of the Juan de Fuca/Gorda plate system and the Pacific plate. This plate convergence is a result of

the Blanco and Mendocino Fracture zones not being parallel which causes a space-problem for the Gorda plate (Figure 1.1). Furthermore, the inferred history of plate tectonics has shown that motion of the Pacific plate has moved the entire Cascadia subduction zone northwestward and will continues to apply this "force" to the Gorda plate. Since the Gorda plate is the youngest, and thus weakest in the system, it is internally deforming under the applied stresses.

Based on the results of relocated hypocenters, it is suggested that the plate boundary between the Pacific and Gorda plate is defined by the trend of the Mattole Canyon fault. Map views of epicenters, cross-sections and focal mechanisms are consistent with the interpretation that interplate activity is expressed as right-lateral translation along the strike of the Mattole Canyon fault. Seismic sections do not reveal any evidence for underthrusting of the Gorda plate beneath the Pacific plate, but provide strong evidence of a near vertical truncation of seismicity. The hypocenters concentrate between 18 and 25 Km depth (Figures 3.11b and 3.12), which is interpreted to be the thickness of the oceanic crust of the Gorda plate beneath Cape Mendocino.

Seismicity patterns and focal mechanisms east of 236°E indicate a change in the stress orientation within the Gorda slab from a north-south compressional to a down-slab extensional [McPherson, 1989]. As the Gorda plate moves past the northeastern edge of the Pacific plate, the "buttressing effect" [Smith et al., 1993] imposed by the Pacific plate is removed (expressed by a termination of seismicity along Mattole Canyon near Punta Gorda), and seismic activity is dominated by normal faulting due

to a negative buoyancy force within the slab. The observed southward dip of seismic activity observed in the two easternmost north-south cross-sections (Figures 3.12d and e) are interpreted to reflect these changes in the orientation of principle stress directions. The distribution of seismicity to the northeast of Cape Mendocino has been shown to define a Wadati-Benioff zone of the subducting Gorda slab.

4.4 Seismic Coupling

The degree of coupling between the subducting Gorda plate and the North America plate is an important factor in the assessment of seismic hazard at the Mendocino triple junction and Northern California in general. The potential for a large earthquake along the megathrust of the Cascadia has been controversial and is closely related to the question whether slip occurs aseismically, as would be expected if the plates are weakly coupled, or seismically in large earthquakes due to a strongly coupled interface.

The comparison of the Cascadia subduction zone to other subduction zones with a history of great earthquakes has been shown to favor both interpretations. Despite good evidence of present-day convergence (see velocity triangle, Figure 1.1), the historic quiescence of the Cascadia subduction zone has been interpreted that plate convergence is accomodated as aseismic slip. Archarya [1992] comes to the conclusion that the low rate of earthquake activity throughout the Cascadia subduction zone can be explained on the basis of the combined effect of low rate of plate motion, significant

aseismic subduction, and young age of the lithosphere. On the other hand, Heaton and Kanamori [1984] interpret the lack of subduction related earthquakes, the young age of the subducted plate and the shallow dip of the subduction zone as indications that the interface is locked.

Before 1992, the absence of any historic large subduction related earthquakes along the Cascadia subduction zone seemed to favor the interpretation of aseismic subduction of the Gorda plate. However, the occurence of the 1992 Cape Mendocino thrust earthquake ended the historic quiescence in seismicity along the Cascadia subduction zone as this event is interpreted to have relieved strain due to Gorda and North America plate convergence. Furthermore, the triggering of two M=6.6 aftershocks in the subducting Gorda plate (chapter 3.3.5) suggests significant coupling of stresses between the converging plates. The mainshock was also followed by extensive shallow seismicity near Cape Mendocino that was associated with strain relieve within the southern forearc contractional zone. However, Oppenheimer et al. [1993] note that the 1992 Cape Mendocino earthquake may not be typical of other Cascadia subduction zone earthquakes due to the structural complexity in the region of the main shock, yet paleoseismic studies [Merrits, 1996; Clarke and Carver, 1992] suggest a history of large subduction related events in the past.

The results of this study are supportive of an interpretation that subduction of the Gorda plate beneath North America should be accompanied by large thrust earthquakes. The scattered distribution of seismicity within the contractional fore-

arc region of the North America plate, the occurence of the 1992 Cape Mendocino earthquake with triggered aftershocks in the Gorda plate, and earthquakes with extensional mechanisms within the Wadati-Benioff zone suggest that plate motion is being resisted at the shallow subduction interface due to strong coupling. Thus, the potential for a M 8.0-8.5 earthquake along the Cascadia subduction zone exists, with the Mendocino triple junction possibly marking the southern extent in rupture.

4.5 Conclusions

The region at the Mendocino triple junction is characterized by a high level of seismicity, reflecting the complex active tectonics associated with the junction of the Pacific, North America and Gorda plates. From the hypocentral distribution of more than 6000 earthquakes, a large-scale three-dimensional structure is inferred.

The intense seismic activity offshore Cape Mendocino is bounded to the south along the trend of the Mattole Canyon fault. This truncation of seismicity is near vertical in cross-sections and marks the plate boundary of the Pacific plate. The observed double seismic zone along this boundary is interpreted as the transform boundary to the North America and Gorda plates at depths less than 12 Km and greater than 18 Km, respectively. This interpretation implies that the Mendocino triple junction is located offshore, which is contrary to earlier proposals that it may be situated onshore southeast of Cape Mendocino.

The majority of earthquakes at the Mendocino triple junction are located within

the Gorda plate and reflect the internal deformation on NE-SW and NW-SE trending faults in reponse to north-south compression. From the intense intraplate seismicity, it is inferred that the Gorda slab is located at depths greater than 18 Km beneath Cape Mendocino and dips gently to the east. Once the Gorda plate passes the obstruction imposed by the northeastern corner of the Pacific plate, a southward dip in seismicity and focal mechanisms indicate a change to an extensional stress regime indicative of a slab pull force.

The 1991 Honeydew and 1992 Cape Mendocino earthquakes are both interpreted to have occured on blind thrust faults within the accretionary wedge of the Cascadia subduction zone. Large aftershocks of the 1992 event in the Gorda plate and scattered seismicity within the contractional forearc region near Cape Mendocino are consistent with an interpretation of a strongly coupled Cascadia subduction zone, capable of producing a M 8 earthquake.

The analysis of seismicity patterns has shown that active tectonics at the Mendocino triple junction are continuing into the present and will continue to play an important role in the geological evolution of western North America. The use of a one-dimensional velocity model in the earthquake location model has been shown to provide reliable, relative locations of hypocenters in the region. Based on the results of this study, the application of a three-dimensional velocity model in the location procedure is recommended for the future to further improve the quality of hypocentral parameters. Future work should also include a local travel time tomography of

the Mendocino triple junction region with the goal of imaging the three-dimensional seismic velocity structure.

References

Archarya, H., 1992, Comparison of Seismicity Parameters in Different Subduction Zones and its Implications for The Cascadia Subduction Zone: J. Geophys. Res., **97**, no. B6, 8831–8842.

Atwater, T., and Molnar, P., 1973, Relative motion of the Pacific and North American plates deduced from sea-floor spreading in the Atlantic, Indien, and South Pacific Oceans: Proceedings of the Conference on Tectonic Problems of the San Andreas fault system, **13**, 136–148.

Atwater, T., 1970, Implications of plate tectonics for the Cenozoic tectonic evolution of Western North America: Geol. Soc. Am. Bull., **81**, 3513–3536.

Benz, H. M., Zandt, G., and Oppenheimer, D. H., 1992, Lithospheric structure of northern California from teleseismic images of the upper mantle: J. Geophys. Res., **97**, no. B4, 4791–4807.

Bolt, B. A., Lomnitz, C., and McEvilly, T. V., 1968, Seismological evidence on the tectonics of central and northern California and the Mendocino escarpment: Bull.

Seism. Soc. Am., **58**, no. 6, 1725–1767.

Carlson, R. L., 1976, Cenozoic plate convergence in the vicinity of the Pacific Northwest: A Synthesis and assessment of plate tectonics in the northeastern Pacific: Ph.D. thesis, Univ. of Wash., Seattle.

Carlson, R. L., 1981, Late Cenozoic rotations of the Juan de Fuca Ridge and the Gorda Rise: A case study: Tectonophysics, **77**, 171–188.

Castillo, D. A., and Ellsworth, W. L., 1993, Seismotectonics of the San Andreas Fault System between Point Arena and Cape Mendocino in Northern California: Implications for the Development and Evolution of a young Transform: J. Geophys. Res., **98**, no. B4, 6543–6560.

Clarke, S. H., and Carver, G. A., 1992, Late Holocene tectonics and paleoseismicity, southern Cascadia subduction zone: Science, **255**, 188–192.

Clarke, S. H., 1992, Geology of the Eel River Basin and adjacent region; implications for late Cenozoic tectonics of the southern Cascadia subduction zone and Mendocino triple junction: American Association of Petrolium Geologists Bulletin, **76**, no. 2, 199–224.

Cockerham, R. W., Smith, S. W., and McPherson, R. C. Earthquake epicenters and selected fault plane solutions for the Northern California continental margin (with

geologic structure):. in California Continental Margin Geological Map Series, 1989. *Map7B*, Calif. Div. of Mines and Geol.

Cockerham, R. S., 1984, Evidence for 180-Km-long subducted slab beneath northern California: Bull. Seism. Soc. Am., **74**, no. 2, 569–576.

DeMets, C., Gordon, R. G., Argus, D. F., and Stein, S., 1990, Current plate motions: Geophys. J. Int., **101**, 425–478.

Dengler, L., Carver, G., and McPherson, R., 1992, Sources of North Coast Seismicity: California Geology, **45**, 40–53.

Dickinson, W. R., and Snyder, W. S., 1979, Geometry of triple junctions related to San Andreas transfom: J. Geophys. Res., **84**, no. B2, 561–572.

Dreger, D. S., and Romanowicz, B., 1994, Source Characteristics of Events in the San Francisco Bay Region: USGS Open-file report, , no. 94-176, 301–309.

Dreger, D. S. UC Berkeley Seismological Laboratory Seismic Moment Tensor catalog:. at *http://www.seismo.berkeley.edu/ dreger/mtindex.html*, 1998.

Dziewonski, A. M., Ekström, G., and Salganik, M. P., 1992, Centroid-moment-tensor solutions for July-September 1991: Phys. Earth Planet. Inter., **72**, 1–11.

Dziewonski, A. M., Ekström, G., and Salganik, M. P., 1993, Centroid-moment-tensor solutions for April-June 1992: Phys. Earth Planet. Inter., **77**, 151–163.

Eaton, J. P., 1981, Detailed study of the November 8, 1980, Eureka, California earthquake and its aftershocks (abstract): EOS Trans. AGU, **62**, no. 45, 959.

Furlong, K. P., Hugo, W. D., and Zandt, G., 1989, Geometry and evolution of the San Andreas Fault Zone in Northern California: J. Geophys. Res., **94**, no. B3, 3100–3110.

Gee, L. S., Uhrhammer, R. A., and Romanowicz, B., 1991, Source parameters and rupture characteristics of the Gorda basin earthquakes and their tectonic implications (abstract): EOS Trans. AGU, **72**, no. Fall Meet. Suppl., 312.

Graham, S. A., and Dickinson, W. R., 1978, Evidence for 115 kilometers of right-slip on the San Gregorio- Hosgri fault trend: Science, **199**, 179–181.

Griscom, A., and Jachens, R. C., 1989, Tectonic History of the North Portion of the San Andreas Fault System, California, Inferred from Gravity and Magnetic Anomalies: J. Geophys. Res., **94**, no. B3, 3089–3099.

Heaton, T. H., and Kanamori, H., 1984, Seismic potential associated with subduction in the northwestern United States: Bull. Seis. Soc. Am., **74**, 933–941.

Hill, M. L., and Dibblee, T. W., 1953, San Andreas, Garlock, and Big Pine faults, California–a study of the character, history, and tectonic significance of their displacements: Bull. Geol. Soc. Amer., **64**, no. 4, 443–458.

Jachens, R. C., and Griscom, A., 1983, Three-dimensional geometry of the Gorda plate beneath northern California: J. Geophys. Res., **88**, no. B11, 9375–9392.

Kelsey, H. M., and Carver, G. A., 1988, Late Neogene and Quaternary Tectonics associated with northward growth of the San Andreas Transform Fault, Northern California: J. Geophys. Res., **93**, no. B5, 4797–4819.

McKenzie, D. P., and Morgan, W. J., 1969, Evolution of triple junctions: Nature, **224**, 125–133.

McLaughlin, R. J., Sliter, W., Frederikson, N. O., Harbert, W. P., and McCulloch, D. S., 1994, Plate Motions recorded in Tectonostratigraphic Terranes of the Franciscan Complex and Evolution of the Mendocino Triple Junction, Northwest California: U.S. Geol. Surv. Bull, **1994**, 60pp.

McPherson, R. C., and Dengler, L. A., 1992, The Honeydew Earthquake August 17, 1991: California Geology, **45**, 31–39.

McPherson, R. C., 1989, Seismicity and focal mechanisms near Cape Mendocino, northern California: 1974-1984: Master's thesis, Humboldt State University.

Merrits, D. J., 1996, The Mendocino triple junction: Active faults, episodic coastal emergence, and rapid uplift: J. Geophys. Res., **101**, no. B3, 6051–6070.

Murray, M. H., Marshall, G. A., Lisowski, M., and Stein, R. S., 1996, The 1992 M=7 Cape Mendocino, California, earthquake: Coseismic deformation at the south end of the Cascadia megathrust: J. Geophys. Res., **101**, no. B8, 17707–17725.

Ogle, B. A., 1953, Geology of the Eel River valley area, Humboldt County,California: Calif. Div. of Mines Bull., **164**, 128 pp.

Oppenheimer, D. H., and Eaton, J. P., 1984, Moho orientation beneath central California from regional earthquake travel times: J. Geophys. Res., **89**, no. B12, 10267–10282.

Oppenheimer, D. H., and Magee, M. E., 1991, The 1991 M6.0 Honeydew, California, earthquake (abstract): EOS, Trans. AGU, Fall Meet. Suppl., **72**, 311–312.

Oppenheimer, D., Beroza, G., Carver, G., Dengler, L., Eaton, J., Gee, L., Gonzales, F., Jayko, A., Li, W. H., Lisowski, M., Magee, M., Marshall, G., Murray, M., McPherson, R., Romanowicz, B., Satake, K., Simpson, R., Somerville, P., Stein, R., and Valentine, D., 1993, The Cape Mendocino, California, earthquakes of April 1992: Subduction at the Triple Junction: Science, **261**, 443–438.

Pasyanos, M. E., Dreger, D. S., and Romanowicz, B., 1996, Towards Real-Time Determination of Regional Moment Tensors: Bull. Seism. Soc. Am., **86**, 1255–1269.

Raff, A. D., and Mason, R. G., 1961, Magnetic survey off the west coast of north America, 40° N latitude to 50° N latitude: Geol. Soc. Am. Bull., **72**, 1267–1270.

Riddihough, R. P., 1980, Gorda plate motions from magnetic anomaly analysis: Earth Planet. Sci. Lett., **51**, 163–170.

Riddihough, R. P., 1984, Recent movements of the Juan de Fuca plate system: J. Geophys. Res., **89**, no. B8, 6980–6994.

Romanowicz, B. A., 1980, Large scale three-dimensional P velocity structure beneath western U.S. and the lost Farallon plate: Geophys. Res. Lett., **7**, 345–348.

Silver, E. A., 1971, Tectonics of the Mendocino Triple Junction: Geol. Soc. Am. Bull., **82**, 2965–2978.

Simila, G. W., Peppin, W. A., and McEvilly, T. V., 1975, Seismotectonics of the Cape Mendocino, California, Area: Geol. Soc. Am. Bull., **86**, 1399–1406.

Smith, S. W., and Knapp, J. S., 1980, The northern termination of the San Andreas fault zone in northern California: Spec. Rep. Calif. Div. of Mines Geol., **140**, 153–164.

Smith, S. W., McPherson, R. C., and Severy, N. I. The Eureka earthquake of 1980, break-up of the Gorda plate:. Paper presented at Seismological Society of America Meeting, Berkeley, Calif., 1981.

Smith, S. W., Knapp, J. S., and McPherson, R. C., 1993, Seismicity of the Gorda plate, structure of the continental margin, and an eastward jump of the Mendocino Triple junction: J. Geophys. Res., **98**, no. B5, 8153–8171.

Smith, S. W., Humboldt Bay Seismic Network annual report, August 1974-August 1975:, Technical report, TERA Corp., 1975.

Spence, W., 1989, Stress origins and earthquake potentials in Cascadia: J. Geophys. Res., **94**, no. B3, 3076–3088.

Stanley, R. G., 1987, New Estimates of displacement along the San Andreas fault in central California based on paleobathymetry and paleogeography: Geology, **15**, 171–174.

Taber, J., and Smith, S. W., 1984, Seismicity and focal mechanisms associated with the subduction of the Juan de Fuca plate beneath the Olympic Peninsula, Washington.: Bull. Seis. Soc. Am., **75**, no. 1, 237–250.

Velasco, A. A., Ammon, C. J., and Lay, T., 1994, Recent large earthquakes near Cape Mendocino and in the Gorda plate: Broadband source time functions, fault orientations, and rupture complexities: J. Geophys. Res., **99**, no. B1, 711–728.

Verdonck, D., and Zandt, G., 1994, Three-dimensional crustal structure of the Mendocino Triple Junction region from local earthquake travel times: J. Geophys. Res., **99**, no. B12, 23843–23858.

Weaver, C. S., and Michaelson, C. A., 1985, Seismicity and volcanism in the Pacific northwest: Evidence for the segmentation of the Juan de Fuca plate: Geophys. Res. Lett., **12**, 215–218.

Wilson, D. S., 1986, A kinematic model for the Gorda deformation zone as a diffuse southern boundary of the Juan de Fuca plate: J. Geophys. Res., **91**, no. B10, 10259–10269.

Wilson, D. S., 1989, Deformation of the so-called Gorda plate: J. Geophys. Res., **94**, no. B3, 3065–3075.

Appendix A

Station Data

The following tables contain information on the station locations and applied station corrections for S- and P-phases. Station corrections are calculated for stations that recorded a minimum of five (5) phases for events of a high-quality subset. The period of operation is given as yymm-yymm.

Table A.1: Station locations and applied stations corrections

Station	Latitude N	Longitude W	Elevation [m]	S-cor. [s]	P-cor. [s]	period of operation
GBD	39°26.5458'	123°18.6392'	632	-0.58	-0.34	7804-9999
GCS	39° 1.3700'	123°31.2700'	695	–	-0.26	8204-8907
GHM	39°29.7271'	122°55.8575'	1456	–	-0.09	7805-9999
GHO	39° 2.6676'	123°32.4653'	671	–	-0.31	8907-9999
GNA	39°11.8502'	123°37.9218'	318	-0.61	-0.30	8104-9999
GRN	39°10.5200'	123°34.5300'	73	–	-0.39	8007-8205
GRO	39°55.0400'	122°40.2300'	1274	–	-0.39	9012-9999

Table A.2: Station locations and applied stations corrections

Station	Latitude N	Longitude W	Elevation [m]	S-cor. [s]	P-cor. [s]	period of operation
GTC	39°23.9665'	123°33.3191'	318	–	-0.24	9607-9999
GWR	39°12.3423'	123°18.0602'	654	–	-0.27	7803-9999
KBB	40°11.8277'	123°51.0912'	538	0.31	0.09	7911-9999
KBN	39°53.5424'	123°11.7018'	1329	0.19	0.32	7911-9999
KBR	40°43.7383'	123°57.2711'	795	-0.16	-0.21	7911-9999
KBS	39°55.0311'	123°35.7365'	1120	0.43	0.04	7911-9999
KCP	39°41.1785'	123°34.9453'	1261	0.19	0.01	8807-9999
KCR	40°25.5865'	123°49.2386'	873	-0.11	-0.05	7911-9999
KCS	40°32.2747'	123°30.8363'	1640	0.43	0.16	9208-9999
KCT	40°28.5500'	124°20.1800'	409	0.35	0.25	7911-9999
KFP	39°38.3331'	123°25.5086'	768	-0.35	-0.21	7911-9999
KGM	40°45.5273'	123°40.4280'	1604	0.23	0.12	7911-9999
KHB	40°39.5941'	123°13.1796'	1864	0.01	-0.16	9111-9999
KHM	40°52.4696'	123°43.9418'	1476	-0.12	-0.03	9107-9999
KIP	39°48.5044'	123°28.8779'	1341	0.21	0.08	8001-9999
KJJ	40°14.8464'	124°18.4962'	693	-0.14	-0.08	9108-9999
KKP	40° 8.7477'	123°28.1789'	1226	0.42	0.43	7912-9999
KMP	40°25.0506'	124°7.2368'	931	-0.43	-0.18	8207-9999
KOM	41°16.7230'	123°27.1889'	1844	-0.11	-0.07	8208-9999
KPP	40°20.7474'	123°21.7967'	1738	0.07	0.24	7911-9999
KRK	39°33.7891'	123°11.0202'	1259	–	0.01	7911-9999
KRM	41°31.3241'	123°54.3767'	1247	-0.45	-0.06	8208-9999
KRP	41° 9.4510'	124°1.4073'	811	-0.19	-0.06	8908-9999
KSC	42°20.6466'	124°9.9304'	1261	–	0.12	9111-9999
KSM	40°11.2084'	124°10.5407'	931	-0.53	-0.16	8208-9999
KSP	39°31.0953'	123°30.0985'	809	–	-0.15	7911-9999
KSX	41°49.8499'	123°52.6062'	1120	-0.46	-0.10	8208-9999
KTR	41°54.5085'	123°22.6528'	1347	–	0.05	9208-9999
LAM	41°36.5920'	122°37.5352'	1769	–	0.12	9501-9999
LBG	40°48.1400'	122°35.3800'	884	–	0.13	8212-8609
LBK	41° 5.0290'	122°40.0388'	1304	0.28	0.02	8212-9999
LBP	40°19.0026'	122°52.9162'	1019	-0.25	-0.09	8212-9999
LGP	40°54.7368'	122°49.7696'	1265	-0.13	-0.10	8210-9999

Table A.3: Station locations and applied stations corrections

Station	Latitude N	Longitude W	Elevation [m]	S-cor. [s]	P-cor. [s]	period of operation
LHO	40°41.1100'	122°45.0000'	1378	0.42	0.11	8212-8609
LPG	40° 8.7200'	122°41.2000'	597	–	0.19	9101-9999
LPK	41°27.3154'	122°32.6231'	1880	–	0.20	9011-9999
LRB	40° 8.5937'	122°33.4628'	308	–	0.53	9012-9999
LSF	40°39.4903'	122°31.4221'	1042	0.18	0.01	8904-9999
LVR	40° 2.3500'	122°40.2500'	963	–	0.33	9101-9999
LWD	40°36.7100'	122°31.6400'	390	–	0.06	8212-8609
ARC	40°52.6200'	124°4.5000'	60	–	–	5206-9301
FHC	40°48.1000'	123°59.1000'	610	–	-0.09	6812-94
WDC	40°34.8000'	122°32.4000'	300	–	–	73 -93
WK2	40°23.3500'	124°17.7300'	976	–	–	8011-8311
WKC	40°23.6000'	124°17.3000'	976	–	-0.34	7610-8011
EU1P	41°44.0800'	124°4.1600'	0	-0.25	-0.03	8011-8012
EU2P	41° 2.8700'	124°6.8500'	0	–	-0.15	8011-8012
EU3P	41° 3.7500'	124°6.3700'	0	-0.06	-0.10	8011-8012
EU4P	41°22.0200'	124°0.8000'	0	–	–	8011-8012
EU5P	41°23.2000'	123°59.8600'	0	–	–	8011-8012
EU6P	40°47.0600'	124°4.0700'	0	-0.45	-0.34	8011-8012
EU7P	40°37.8500'	124°11.1400'	0	0.67	–	8011-8012
EU8P	40°30.9000'	124°0.1600'	0	–	0.09	8011-8012
EU9P	40°57.9200'	123°50.2400'	0	0.06	0.09	8011-8012
EUAP	41°15.5800'	123°38.8500'	0	–	0.05	8011-8012
BRYT	40°43.5300'	123°58.4000'	899	-0.02	-0.07	7406-8607
BZDT	40°31.6200'	124°13.1300'	427	0.42	0.14	7501-8607
DIAT	40°24.8300'	123°45.4500'	533	0.02	-0.05	7406-8607
EKRT	40°41.7200'	124°8.3700'	49	-0.28	-0.23	7406-8607
FKHT	40°47.4500'	123°58.4700'	632	0.01	-0.01	7406-8607
FOXT	40°31.2700'	123°59.5300'	113	0.30	0.08	7406-8607
GWST	40°37.1800'	124°7.8700'	221	0.47	0.11	7406-7806
HAHT	40°33.5300'	123°49.5700'	1091	0.34	0.11	7405-8607
HRST	40°52.5000'	123°43.8700'	899	0.49	0.20	7408-8607
HUMT	40°43.2000'	124°12.4700'	122	0.31	0.15	7610-7806
JBYT	40°49.0200'	124°1.7300'	49	-0.35	-0.20	7408-7602

Table A.4: Station locations and applied stations corrections

Station	Latitude N	Longitude W	Elevation [m]	S-cor. [s]	P-cor. [s]	period of operation
LOLT	40°40.2300'	124°13.7500'	122	0.29	0.15	7406-8607
MMRT	40°25.3500'	124°5.7800'	966	-0.22	-0.19	7407-8607
MVRT	40°40.5300'	123°51.7000'	460	-0.44	-0.27	7406-8607
PRTT	40° 7.2300'	123°41.5000'	1158	0.66	0.34	7807-8607
PTKT	40°36.2700'	124°16.5000'	4	0.46	0.21	7406-8607
RYNT	40°47.1300'	124°7.2200'	4	-0.10	-0.14	7408-8607
TITT	41° 4.4300'	123°58.8200'	641	-0.14	-0.08	7408-8607
WHTT	40° 1.0000'	123°56.2500'	305	-0.11	-0.14	7806-8607
WKRT	40°23.6000'	124°17.2500'	975	-0.05	-0.14	7410-8607
WR2T	40°23.2100'	124°17.4400'	975	0.03	-0.15	74 -8607
GAS	39°39.2900'	122°42.9100'	1231	–	0.13	8006-9999